Organic Geochemistry 102 (2016) 30–44

Contents lists available at ScienceDirect

Organic Geochemistry

journal homepage: www.elsevier.com/locate/orggeochem

Sedimentary alkenone distributions reflect salinity changes in the Baltic Sea over the Holocene

Lisa Warden [a], Marcel T.J. van der Meer [a], Matthias Moros [b], Jaap S. Sinninghe Damsté [a,c,*]

[a] NIOZ Netherlands Institute for Sea Research, Department of Marine Microbiology and Biogeochemistry, and Utrecht University, PO Box 59, 1790 AB Den Burg, The Netherlands
[b] The Leibniz Institute for Baltic Sea Research, Department of Marine Geology, Seestraße 15 D-18119 Rostock, Warnemünde, Germany
[c] Utrecht University, Faculty of Geosciences, P.O. Box 80.021, 3508 TA Utrecht, The Netherlands

ARTICLE INFO

Article history:
Received 8 July 2016
Received in revised form 9 September 2016
Accepted 23 September 2016
Available online 30 September 2016

Keywords:
Alkenones
Baltic Sea
$C_{36:2}$ alkenone
Haptophyte community
Paleosalinity
δD of alkenones

ABSTRACT

The Baltic Sea has had a complex salinity history since the last deglaciation. Here we show how distributions of alkenones and their δD values varied with past fluctuations in salinity in the Baltic Sea over the Holocene by examining a Holocene record (11.2–0.1 cal kyr BP) from the Arkona Basin. Major changes in the alkenone distribution, i.e., changes in the fractional abundance of the $C_{37:4}$ Me alkenone, the $C_{38:2}$ Et alkenone and a $C_{36:2}$ Me alkenone, the latter which has not been reported in the Baltic Sea previously, correlated with known changes in salinity. Both alkenone distributions and hydrogen isotopic composition suggest a shift in haptophyte species composition from lacustrine to brackish type haptophytes around 7.7–7.2 cal kyr BP, corresponding with a salinity change that occurred when the connection between the basin and the North Sea was re-established. A similar salinity change occurred in the Black Sea. Previously published alkenone distributions and their δD values from the Black Sea were used to reconstruct Holocene changes in surface water salinity and, hence, it was shown that the unusual $C_{36:2}$ alkenone dominates the alkenone distribution at salinities of 2–8 ppt (g/kg). This information was used to corroborate the interpretations made about salinity changes from the data presented for the Baltic Sea. Low and variable salinity waters in the Baltic Sea over the Holocene have led to a variable alkenone-producing haptophyte community composition, including low salinity adapted species, hindering the use of the unsaturation ratios of long-chain alkenones for sea surface temperature reconstruction. However, these alkenone based indices are potentially useful for studying variations in salinity, regionally as well as in the past.

1. Introduction

Long chain alkenones, biolipids composed of predominantly C_{37}–C_{39} *n*-alkyl chains with di-, tri- or tetra unsaturations and a keto functionality at position C-2 or C-3 (de Leeuw et al., 1980; Volkman et al., 1980; Rechka and Maxwell, 1988) are produced exclusively by only a few species of haptophyte algae in both open marine (i.e., *Emiliania huxleyi* and *Gephyrocapsa oceanica*; Volkman et al., 1980, 1995; Group III following the phylogenetic classification of Theroux et al., 2010) and coastal marine or lacustrine settings (i.e., algae of the genera *Isochrysis*, *Ruttnera* (formerly *Chrysotila*) and *Tisochrysis*; Marlowe et al., 1984; Nakamura et al., 2016; Group II) and the more recently discovered 'Greenland haptophyte' species, so far exclusively found in Greenland and Alaskan lakes (D'Andrea et al., 2006; Longo et al., 2016; Group I). This latter group has a distinctly different alkenone distribution relative to the alkenones produced by all other haptophytes since they all contain tri-unsaturated alkenone isomers not observed in these other species (Dillon et al., 2016; Longo et al., 2016). An unusual C_{36} diunsaturated alkenone was identified by Xu et al. (2001) in Holocene sediments from the Black Sea. Coolen et al. (2009) reported that it was derived from a specific strain of *E. huxleyi* based on the analysis of fossil DNA.

Since field sampling and culture experiments demonstrated a relationship between surface water temperature and the unsaturation ratios of long-chain alkenones (Prahl and Wakeham, 1987; Müller et al., 1998), the unsaturation ratios of sedimentary alkenones have been extensively used as a paleotemperature proxy in marine settings. Two alkenone unsaturation ratios have been predominantly used in sea surface temperature (SST) reconstructions, the U^K_{37} (which includes the relative abundance of di-, tri- and tetra-unsaturated alkenones; Brassell et al., 1986) and the

* Corresponding author at: NIOZ Netherlands Institute for Sea Research, Department of Marine Microbiology and Biogeochemistry, and Utrecht University, PO Box 59, 1790 AB Den Burg, The Netherlands.
E-mail address: jaap.damste@nioz.nl (J.S. Sinninghe Damsté).

http://dx.doi.org/10.1016/j.orggeochem.2016.09.007
0146-6380/

$U^{K'}_{37}$ (which excludes the tetra-unsaturated alkenone; Prahl and Wakeham, 1987). Even though this proxy has been successfully applied in marine settings, uncertainties still exist due to increasing evidence of non-thermal effects on alkenone distribution patterns such as species and strain composition (Volkman et al., 1995; Conte et al., 1998) and salinity (Chu et al., 2005; Ono et al., 2012; Chivall et al., 2014). For example, Rosell-Melé (1998) demonstrated that the amount of $C_{37:4}$ alkenone compared to the abundance of the other C_{37} alkenones (%$C_{37:4}$) in particulate organic matter from Nordic seas had a stronger correlation to sea surface salinity (SSS) than SST. Despite these results, the correlation between salinity and%$C_{37:4}$ in surface water and sediment trap samples worldwide varies greatly and so there is no evidence supporting the application of a linear relationship (Sikes and Sicre, 2002), which would make the use of%$C_{37:4}$ as a salinity proxy possible.

Alkenones are common biomarkers in marine sediments, but they also occur in lake sediments (e.g., Cranwell, 1985; Volkman et al., 1988; Thiel et al., 1997; Zink et al., 2001; Chu et al., 2005; Sun et al., 2007; Nelson and Sachs, 2014; Randlett et al., 2014; Song et al., 2016) although they are not as widespread. In these lake settings, complications applying long chain alkenone unsaturation patterns as a temperature proxy have often been noted. Alkenone-biosynthesizing haptophyte algae are much more genetically diverse in lacustrine settings than marine (e.g., Coolen et al., 2004; Theroux et al., 2010; Randlett et al., 2014) and this affects alkenone composition and has implications for lake surface temperature (LST) reconstruction since alkenone calibrations for Group I and II Isochrysidales vary substantially (e.g., Versteegh et al., 2001; Theroux et al., 2013; Nakamura et al., 2014, 2016; Longo et al., 2016). In many lakes the fractional abundance of the $C_{37:4}$ methyl ketone is much higher (up to 96% of the sum of C_{37} alkenones) than has been observed in marine settings (e.g., Chu et al., 2005; Nelson and Sachs, 2014). The predominance of the $C_{37:4}$ methyl ketone and the observed negative relationship with salinity suggested that its production may be a response to low salinity conditions (Chu et al., 2005; Song et al., 2016). Consequently, it was suggested that the long chain alkenone unsaturation ratio omitting $C_{37:4}$ ($U^{K'}_{37}$) may yield more accurate LST/SST estimations when used in lacustrine, brackish and estuarine waters. However, it is more likely that salinity influences the haptophyte composition, in turn affecting alkenone distributions, i.e., in freshwater in freshwater and oligohaline lakes Group I Isochrysidales dominate and their alkenone distribution is dominated by the $C_{37:4}$ alkenone (Toney et al., 2012). Based on this finding, a new temperature index has been proposed for lacustrine, brackish and estuarine settings that includes the $C_{37:4}$ alkenone and instead excludes $C_{37:2}$ ($U^{K''}_{37}$; Zheng et al., 2016). This study suggested that the di-unsaturated alkenones play a less important role than the tri- and tetra-unsaturated alkenones in regards to regulating cell functions in accordance with temperature fluctuations in lower salinity settings.

Previous studies of alkenones in brackish settings have shown that since alkenone distributions co-vary with salinity-driven changes in haptophyte species composition, the use of long chain alkenones is complicated in areas with low and/or fluctuating salinity such as in the Black Sea (Coolen et al., 2009), Ace Lake in Antarctica (Coolen et al., 2004), the Baltic Sea (Rosell-Melé, 1998; Schulz et al., 2000; Blanz et al., 2005) and the North Atlantic and Nordic seas (Rosell-Melé, 1998). In Ace Lake, Coolen et al. (2004) demonstrated that as lake chemistry changed over time, particularly the salinity as it evolved from a freshwater basin to a marine inlet, the alkenone distributions changed reflecting differences in the haptophyte population as evident from paleogenetic signatures. Similarly, in the Black Sea, Coolen et al. (2009) showed that as salinity increased over the Holocene in the basin, the haptophyte composition changed as well resulting in erroneous alkenone-derived SST estimates at times.

Culture experiments indicate that alkenone distribution patterns can vary with changing salinity and that this should be taken into account when using the alkenone unsaturation indices for SST reconstructions (Chu et al., 2005; Ono et al., 2012; Chivall et al., 2014). The results from Chivall et al. (2014) indicate salinity has an effect on alkenone distributions, but that other factors such as growth phase and species composition also play a role in whether the long chain alkenone distributions are affected by salinity. This culture study found a positive correlation between%$C_{37:4}$ and salinity, however, they found that growth phase has a larger effect on the%$C_{37:4}$ than salinity. Further complicating the use of long chain alkenones for SST and LST reconstructions, Ono et al. (2012) established using culture experiments that salinity had an effect on alkenone unsaturation ratios at 20 °C, but not at 15 °C.

In addition to looking at alkenone distributions to infer salinity changes, culture studies have shown the hydrogen isotopic composition (δD) of long chain alkenones strongly depends on salinity as well in batch culture (Schouten et al., 2005) and recently also in continuous culture where salinity was the environmental parameter that was changed (Sachs et al., 2016). M'boule et al. (2014) also found a strong linear relationship between δD and salinity in culture experiments involving both *I. galbana* (a coastal species) and *E. huxleyi* (an open ocean species), suggesting that δD of alkenones might indeed be used to reconstruct relative shifts in paleosalinity. However, coastal species, such as *I. galbana* and *Ruttnera (Chrysotila) lamellosa*, have been observed to fractionate almost 100‰ less against deuterium than more open marine species, such as *E. huxleyi* and *G. oceanica*, in culture (Schouten et al., 2005; Chivall et al., 2014; M'boule et al., 2014). The δD of sedimentary alkenones might therefore also be indicative of specific alkenone producing haptophytes.

The present day Baltic Sea has a large range in salinities (~3.5–32 ppt or g/kg), with fresher water in the northeastern part of the basin (including the Gulf of Bothnia and Gulf of Finland) and saltier water closer to the connection to the North Sea, making it an interesting site to study present-day salinity effects on alkenone production. Schulz et al. (2000) demonstrated that alkenone unsaturation ratios in surface sediments of the Baltic Sea have a low correlation to mean annual SST and instead primarily reflect salinity changes. The authors postulate that lower salinity in parts of the basin causes salinity stress induced changes in alkenone biosynthesis. This, together with the production of alkenones by haptophytes adapted to lower salinities, results in distinct alkenone patterns with lower salinity regions of the basin having patterns more characteristic of freshwater haptophytes or a mixture of freshwater and marine haptophytes, and saltier regions having distributions that resemble more marine haptophyte derived alkenones. Blanz et al. (2005) also reported that in the Baltic Sea salinity-induced stress on *E. huxleyi* could alter the biosynthesis of alkenones, thus affecting the use of the alkenone unsaturation ratios as a proxy for SSTs. The absence of C_{38} methyl ketones observed in lower salinity water masses in the Baltic Sea has been observed in Chinese Lakes as well (Song et al., 2016). This may be an indication for the presence of brackish alkenone producers of the Group II Isochrysidales. However, it should be noted that the freshwater and oligohaline species of the Group I Isochrysidales do produce C_{38} methyl ketones like *E. huxleyi* (Toney et al., 2012; Zheng et al., 2016).

Here we determine how alkenone distributions and concentrations, along with the δD of alkenones, varied with past changes in salinity in the Baltic Sea over the Holocene. Not only does salinity vary regionally over the Baltic Sea basin today, but the Baltic Sea also has had a complex salinity history since the last deglaciation

and has gone through two fresh water and two brackish water stages (see Section 2.1 for more details). In this study we examined a Holocene record from the Arkona Basin to determine if changes in alkenone distribution patterns that exist today and correlate with salinity around the basin also existed in the past and co-varied with historical salinity changes.

2. Methods

2.1. Historical setting of the Baltic Sea and description of the study site

The Baltic Sea (Fig. 1) is the world's largest brackish body of water with an area of about 377,000 km^2 that is partitioned into multiple sub-basins. The Baltic is almost entirely enclosed by land with a large freshwater contribution (including precipitation) of 660 km^3/yr from a drainage basin that is 1.6 million km^2 (Björck, 1995). An inflow of 475 km^3/yr of saltwater pours in through the only connection to the North Sea, the narrow Straits of Denmark (Tikkanen and Oksanen, 2002). The Baltic Sea is a fairly shallow basin and on average only about 54 m deep. The salinity varies greatly in the Baltic Sea ranging from ~3.5 ppt in the north to ~8 ppt in the Baltic proper and ~32 ppt in the region where the Baltic connects to the North Sea. A permanent halocline exists at about 13–15 m depth, separating a relatively fresh surface and saline bottom waters.

The development of the Baltic Sea since the last deglaciation has been the focus of many studies in the last decades (Winterhalter, 1992; Björck, 1995; Jensen, 1995; Jensen et al., 1999; Andren et al., 2000). Reasons for such intense scientific interest include the shifting bathymetry, dynamic hydrology and the resulting fluctuating salinity of the Baltic Sea over the Holocene as the basin went through several different phases. Following deglaciation and before its present state, the Baltic Sea transformed from the freshwater Baltic Ice Lake (ca. 12.6–10.3 ka BP) to the slightly brackish Yoldia Sea (ca. 10.3–9.5 ka BP) into the freshwater Ancylus Lake (ca. 9.5–8.0 ka BP) and then into the brackish Littorina Sea (ca. 8.0–3.0 kyr BP) and subsequently into the Post-Littorina Sea/-modern Baltic Sea (Winterhalter, 1992; Björck, 1995; Andren et al., 2000). The Baltic Ice Lake formed as large areas of the southern Baltic basin became ice free. Rapid deglaciation resulted in the uplift of the seabed, bringing the connection of the basin with the North Sea above sea level and causing a large influx of fresh meltwater into the system (Björck, 1995). A climatic cooling resulted in less meltwater and the gradually receding ice sheet allowed drainage of the Baltic Ice Lake to occur, lowering the water level and resulting in a short period of seawater ingression, which characterized the very slightly brackish Yoldia Sea (Björck, 1995; Jensen, 1995). Continued isostatic rebound caused the basin to be once again cut off from the ocean and resulted in the Ancylus Lake (Jensen et al., 1999). Then, at around 8000 years ago, eustatic sea level rise re-opened the connection with the North Sea through the Danish Straits allowing salt water to flow into the Ancylus Lake and transforming it into the brackish Littorina Sea (Winterhalter, 1992). The Ancylus Lake/Littorina Sea transition is a complex period characterized by different phases of brackish-water pulses, initially weak and eventually resulting in fully established brackish conditions (15–20 ppt in the Baltic proper; Hyvärinen et al., 1988) only after ~2000 years (Andren et al., 2000). The Littorina Sea phase, which lasted from ~8000–3000 BP, is characterized by

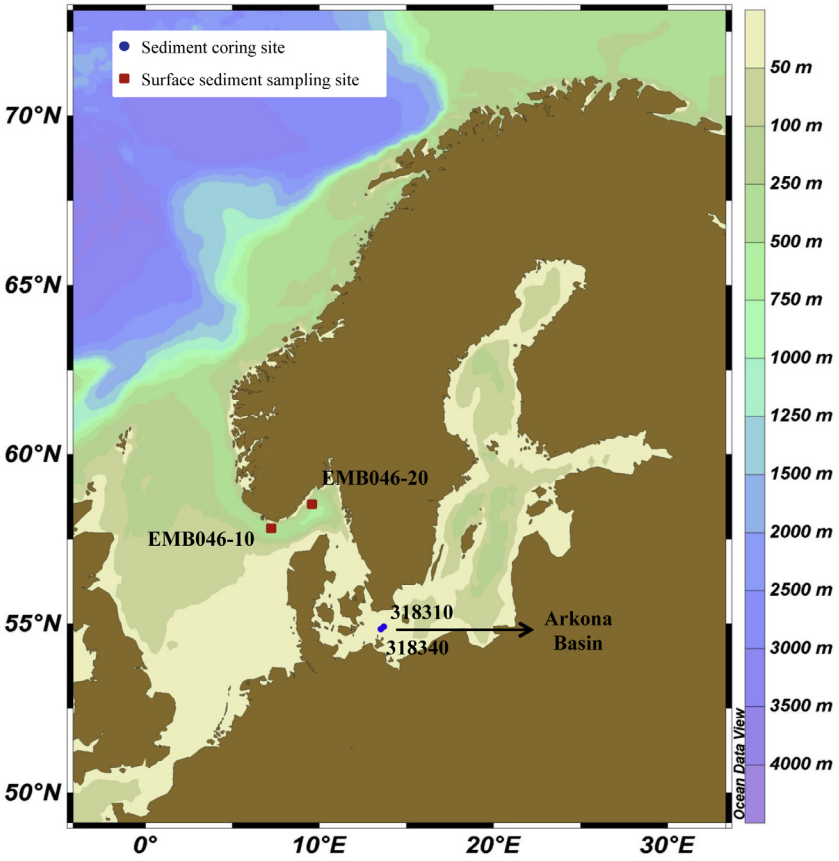

Fig. 1. A map of the Baltic Sea region and sampling sites. The sediment coring sites 318310 and 318340 in the Arkona Basin are designated by blue circles and the two stations in the Skagerrak where surface sediment samples were collected are indicated by red squares. (For interpretation of the references to colour in this figure legend, the reader is referred to the web version of this article.)

a warmer climate and thought to reflect the most marine-like conditions in the Baltic Sea since deglaciation (Andren et al., 2000). The Post-Littorina Sea/modern Baltic Sea are a continuation of the Littorina Sea, but with a salinity thought to be almost half (7–8 ppt in the Baltic proper; Hyvärinen et al., 1988) that of the Littorina Sea (Punning et al., 1988).

2.2. Sampling

Two sediment cores were retrieved from the Arkona Basin, which extends from the Bornholm Basin to the Danish Isles of Falster and Zealand (Fig. 1; Table 1). This basin represents a boundary between the Straits of Denmark, where high salinity water flows in, and the lower salinity Baltic Sea basin. The total discharge of brackish water from the basin is on the order of 950 km^3/yr (Björck, 1995). Both sediment cores were 12 m long and collected using a gravity corer on the R/V "Maria S. Merian" in April of 2006. Sediment core 318310 was recovered at 46 m water depth at 54°50.34′ N and 13°32.03′ E and core 318340 was collected nearby at 54°54.77′ N and 13°41.44′ E at 47 m water depth.

Two surface sediment samples from the Skagerrak obtained using a multi-corer provided a marine end member for comparison with our Baltic Sea sediment core samples. The surface sediment samples were collected during R/V "Elisabeth Mann-Borgese" cruise EMB046 in May 2013. The sampling site for EMB046-10 was positioned at 57°49.74′ N and 07°17.66′ E from 457 m water depth. Site EMB046-20 was situated a bit to the east of EMB046-10 at 58°31.60′ N and 09°29.09′ E from 532 m water depth.

2.3. Loss on ignition (LOI)

The LOI was determined by ashing freeze-dried sediments at 550 °C for 3 h. The resulting mass difference was then calculated in wt%. Previously, it was demonstrated that LOI provides an accurate estimate of the total organic carbon content of the sediments in the Baltic Sea (Leipe et al., 2011). In order to obtain estimates for the total organic carbon (TOC; %) content to normalize the concentration of ketones in the sediments, LOI values were divided by 2.5 (i.e., assuming that the organic matter contains on average 40% C; Dean, 1974).

2.4. X-ray fluorescence (XRF) core scanning

XRF elemental scanning of sediment cores 318310 and 318340 was performed with an Avaatech XRF scanner at a resolution of 0.5 cm.

2.5. Correlation of sediment cores and age model

Sediment cores 318310 and 318340 were correlated to each other on the basis of LOI and XRF-Ca records (Fig. 2). The transition of the Ancylus Lake phase to the Littorina Sea phase is marked by a substantial increase in the TOC content, coinciding with a color change in the sediment (e.g., Moros et al., 2002; Rößler et al., 2011). Just after the large increase in TOC (here reflected in the LOI record), there is a maximum in the carbonate content (here reflected in the maximum in the elemental XRF-Ca record) (Fig. 2), which is caused by the occurrence and preservation of benthic foraminifera (Moros et al., 2002; Rößler et al., 2011). The Ancylus Lake regression is also characterized by a clear peak in the LOI (TC) records, which can be used for correlation purposes (Fig. 2). The transitions, Baltic Ice Lake/Yoldia Sea and Yoldia Sea/Ancylus Lake are revealed by marked changes in the elemental XRF-Ca (carbonate) and bulk density records (Fig. 2; see Moros et al., 2002), and by basin-wide traceable sandy layers (Moros et al., 2002).

Table 1
Alkenone concentrations and distributions in Baltic Sea sediments.

Site	Depth (cm)	Age (cal kyr BP)	Phase[a]	Summed concentration (μg/g TOC)	Fractional abundance							
					$C_{36:2}$ Me	$C_{37:4}$ Me	$C_{37:3}$ Me	$C_{37:2}$ Me	$C_{38:3}$ Et	$C_{38:3}$ Me	$C_{38:2}$ Et	$C_{38:2}$ Me
Skagerrak (EMB0461-10)	0–1	n.d.	n.a.	n.d.	0.00	0.01	0.26	0.20	0.13	0.14	0.20	0.07
Skagerrak (EMB0461-20)	0–1	n.d.	n.a.	n.d.	0.00	0.01	0.27	0.19	0.13	0.14	0.20	0.07
Arkona (core 318310)	20.0	0.1	PL/MB	24	0.13	0.01	0.18	0.17	0.14	0.07	0.24	0.06
	50.0	0.4	PL/MB	32	0.09	0.03	0.23	0.22	0.09	0.09	0.18	0.07
	100.0	0.9	PL/MB (MCA)	156	0.05	0.00	0.10	0.26	0.07	0.05	0.37	0.10
	200.0	1.8	PL/MB	17	0.09	0.02	0.23	0.20	0.12	0.09	0.20	0.06
	300.0	2.7	PL/MB	25	0.11	0.02	0.24	0.20	0.09	0.10	0.17	0.07
	400.0	3.7	LS	2.6	0.56	0.03	0.10	0.05	0.07	0.02	0.09	0.07
	500.0	5.4	LS	2.9	0.57	0.02	0.09	0.06	0.06	0.02	0.11	0.07
	600.0	7.1	LS	5.6	0.38	0.03	0.22	0.13	0.08	0.02	0.11	0.04
	625.0	9.0	AL	3.6	0.00	0.09	0.38	0.10	0.21	0.08	0.11	0.02
	642.5	10.2	AL	3.7	0.01	0.10	0.35	0.09	0.24	0.08	0.10	0.04
Arkona (core 318340)	400.5	7.3	AL/LS TP	16	0.07	0.02	0.23	0.06	0.31	0.02	0.27	0.02
	420.5	7.4	AL/LS TP	42	0.01	0.03	0.49	0.13	0.15	0.02	0.17	0.01
	440.5	7.5	AL/LS TP	6.0	0.02	0.13	0.38	0.11	0.15	0.10	0.09	0.02
	464.5	7.6	AL/LS TP	4.8	0.00	0.10	0.37	0.10	0.11	0.06	0.16	0.10
	480.5	7.7	AL/LS TP	6.9	0.11	0.08	0.28	0.11	0.22	0.05	0.12	0.02
	500.5	8.0	AL	8.1	0.04	0.09	0.37	0.10	0.20	0.07	0.12	0.02
	520.5	8.5	AL	0.0	n.a.	n.a.	n.a.	n.a.	n.a.	n.a.	n.a.	n.a.
	540.5	8.9	AL	15	0.00	0.09	0.35	0.11	0.19	0.11	0.13	0.02
	584.5	9.9	AL	55	0.00	0.04	0.36	0.14	0.25	0.07	0.11	0.03
	643.5	10.3	AL	n.d.	n.a.	n.a.	n.a.	n.a.	n.a.	n.a.	n.a.	n.a.
	705.5	10.5	AL	n.d.	0.00	0.04	0.24	0.12	0.27	0.05	0.25	0.03
	750.5	10.6	AL	n.d.	0.01	0.03	0.30	0.09	0.33	0.02	0.21	0.01
	800.5	10.9	YS	n.d.	n.a.	n.a.	n.a.	n.a.	n.a.	n.a.	n.a.	n.a.
	840.5	11.2	YS	n.d.	n.a.	n.a.	n.a.	n.a.	n.a.	n.a.	n.a.	n.a.

n.a. = not applicable; n.d. = not determined because TOC content for these sediments was not measured.
[a] PL/MB = post Littorina/modern Baltic, MCA = Medieval Climatic Anomaly, LS = Littorina Sea, TP = transitional phase, AL = Ancylus Lake, YS = Yoldia Sea.

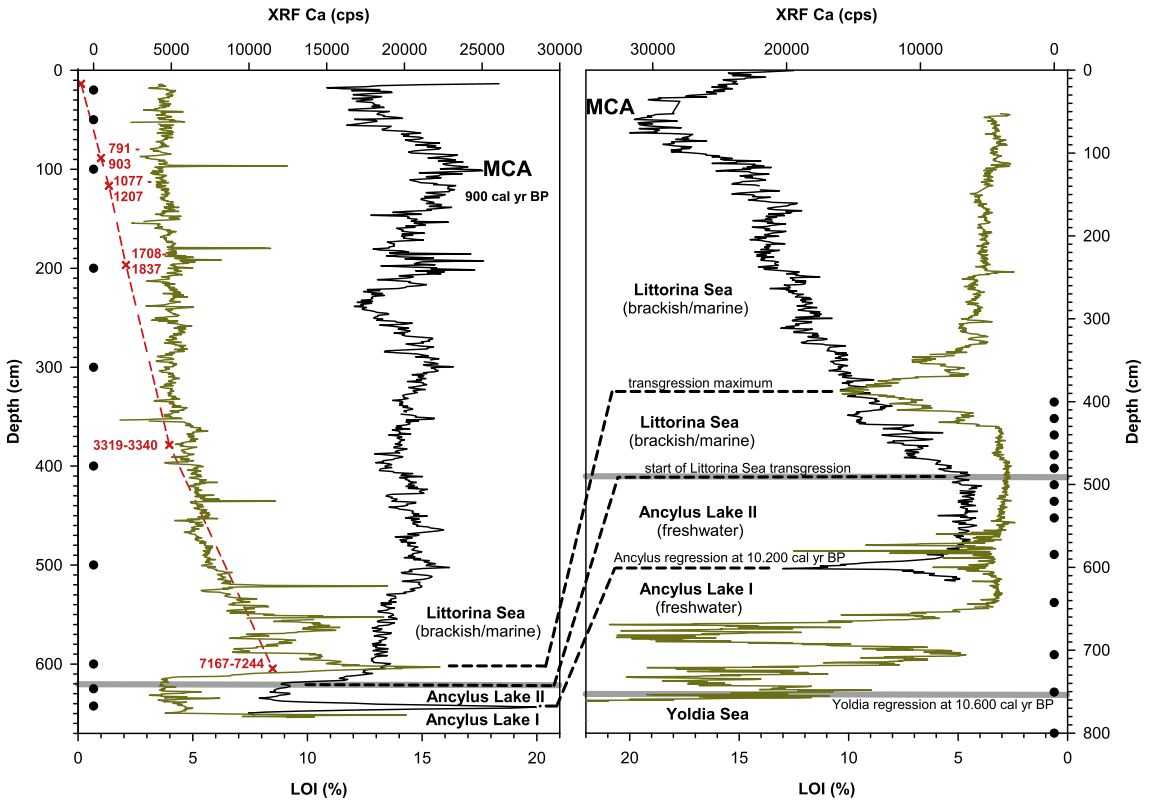

Fig. 2. Correlation of sediment cores 318310 (left panel) and 318340 (right panel; note reversed *X*-axes) using Ca data obtained from XRF analysis (cps; designated by the gold line) and LOI (wt%; designated by the black line). The red numbers indicate the radiocarbon dates (in cal yr BP) of carbonate fossils from specific horizons in core 318310. The dashed black lines indicate tie points used for correlating both cores (see text). The closed circles along the depth axes indicate the positions of the sediments analyzed for alkenones in this study. Stage boundaries between lithostratigraphic units according to Moros et al. (2002) are indicated with gray horizontal lines. MCA denotes the Medieval Climate Anomaly. (For interpretation of the references to colour in this figure legend, the reader is referred to the web version of this article.)

The age model for sediment core 318310 is based on a previous AMS ^{14}C date (7.2 cal kyr BP) on *Mytilus edulis* close to the base of the Littorina phase (Rößler et al., 2011) and five additional dates on mollusc shells (Fig. 2). The age model of the section of sediment core 318340 that was studied (400–840 cm) is based on the carbonate maximum at 380 cm (7.2 cal kyr BP; Moros et al., 2002; Rößler et al., 2011). The start of the Ancylus Lake/Littorina Sea transitional phase at 7.7 cal kyr BP (unpublished results) is revealed by the increase in the LOI record at 485 cm, and the Ancylus Lake regression at 10.2 cal kyr BP is denoted by the sharp peak in the LOI record (sandy layer; Moros et al., 2002) at 600 cm. The boundary between the Yoldia Sea phase and the Ancylus Lake phase (10.6 cal kyr BP; Moros et al., 2002) at 768 cm.

2.6. Lipid extraction and analysis

The sediments were freeze dried and ground and homogenized by mortar and pestle for extraction. In general, 1–3 g of sediment was extracted using a Dionex™ accelerated solvent extractor with dichloromethane/methanol (9:1; v:v) as extraction solvent. The total lipid extract was dried over a Na_2SO_4 column and then separated into three fractions using Al_2O_3 column chromatography: apolar (eluted with 9:1 v:v hexane/DCM), ketone (1:1 v:v hexane/DCM) and polar (1:1 v:v DCM/MeOH) fractions. The ketone fraction was then base hydrolyzed by refluxing the dry fraction in a 1 N KOH in MeOH solution for 1 h after which the pH was adjusted using a 2 N HCl/MeOH solution. DCM was added and the solution was washed twice with DCM. The DCM layers were removed and combined to be dried over a Na_2SO_4 column. After the addition of a nonadecan-10-one internal standard, the alkenone fraction was analyzed using gas chromatography (GC) with an Agilent 6890 instrument equipped with an Agilent CP-Sil 5 CB column (50 m × 0.32 mm i.d.; 0.12 μm film thickness) and a temperature program from 70 °C increasing at 20 °C/min to 200 °C and then at 3 °C/min to 320 °C where it remained for 44 min. Alkenones were identified by GC–mass spectrometry (GC–MS), including the $C_{36:2}$ alkenone, using an Agilent 7890A GC instrument equipped with a Agilent 5975C VL mass selective detector (MSD) and by comparing relative retention times with those of known alkenones from a culture of *E. huxleyi*. Peak areas were used to calculate alkenone unsaturation indices and alkenone concentrations were determined based on peak responses relative to the nonadecan-10-one internal standard.

2.7. Compound specific hydrogen isotope compositions

Alkenone hydrogen isotope analyses were carried out on a subset of the samples, i.e., those containing sufficient amounts of alkenones, on a Thermo Scientific DELTA$^+$ xl GC–TC–irMS. The temperature conditions of the GC increased from 70 to 145 °C at 20 °C/min, then at 8 °C/min to 200 °C and to 320 °C at 4 °C/min, at which it was held isothermal for 20 min. An Agilent CP Sil-5 column (25 m × 0.32 mm) with a film thickness of 0.4 μm was used with helium as carrier gas at 1 ml/min (constant flow). The high temperature conversion reactor was set at 1425 °C. The H_3^+ correction factor was determined daily and was constant at 5.6 ± 0.2 before and 3.8 ± 0.1 after a scheduled power outage and retuning of the irm. A set of standard *n*-alkanes with known isotopic composition (Mixture B prepared by Arndt Schimmelmann, University of Indiana) was analyzed daily prior to analyzing samples in order to

monitor system performance. Samples were only analyzed when the alkanes in Mix B had an average deviation from their off-line determined value of < 5‰. Squalane was co-injected as an internal standard with each sample to monitor the accuracy of the alkenone isotope values. The δD of long chain C_{37} alkenones were measured as the combined C_{37} alkenones ($\delta D_{alkenone}$) (van der Meer et al., 2013) and the same applies to the C_{38} alkenones. The squalane standard yielded an average $\delta D_{alkenone}$ value of -160.7 ± 2.7‰, which is stable, but relatively enriched in D compared to its offline determined δD value of −170‰, potentially due to co-eluting compounds in this sample set.

2.8. Calculation of alkenone based proxies

$\%C_{37:4}$ is the contribution of the tetra-unsaturated 37-carbon methyl alkenone ($C_{37:4}$) to total C_{37} alkenone concentrations and calculated according to Rosell-Melé (1998):

$$\%C_{37:4} = C_{37:4}/(C_{37:2} + C_{37:3} + C_{37:4}) \times 100 \quad (1)$$

The U^K_{37} index represents the relative abundance of the diunsaturated ($C_{37:2}$), triunsaturated ($C_{37:3}$) and tetraunsaturated ($C_{37:4}$) methyl ketones (Brassell et al., 1986). Later, the tetraunsaturated methyl ketone ($C_{37:4}$) was removed from the equation because this compound was rarely found in open-sea sediments or suspended water column particles and the equation was modified by Prahl and Wakeham (1987):

$$U^{K'}_{37} = C_{37:2}/(C_{37:2} + C_{37:3}) \quad (2)$$

2.9. Statistical analysis

Utilizing the R software package for statistical analysis, principal component analysis (PCA) based on the correlation matrix was executed on the fractional abundances of the eight alkenones quantified in the sediments studied. Four sediment samples from sediment core 318340 with no alkenones present were omitted from the PCA.

3. Results

3.1. Phases of the Baltic Sea covered in the Arkona Basin record

The XRF (Ca) and LOI (TC) data were used to distinguish different phases captured by each sediment core in this study (Fig. 2) and to correlate the two sediment cores (see Methods). The sedimentary record for sediment core 318310 covers the upper section of the freshwater Ancylus Lake stage starting at 10.2 cal kyr BP (642.5 cm), but mostly spans the brackish phase of the basin beginning from 7.1 cal kyr BP (600–20 cm) (Fig. 2a). From sediment core 318310 we studied eight sediment samples representing the brackish phase including the Littorina Sea and post-Littorina Sea/-modern Baltic Sea stage and two samples representing the Ancylus Lake stage (Fig. 2a; Table 1). To obtain more information on alkenone occurrence and distribution during the Ancylus Lake stage, we also studied samples from another sediment core. This core (318340) includes the Yoldia Sea stage (11.2–10.6 cal kyr BP; 840.5–780.5 cm), the Ancylus Lake stage (10.6–7.8 cal kyr BP; 750.5–500.5 cm), and the Littorina Sea and post-Littorina Sea/modern Baltic Sea stage (7.2–0.1 cal kyr BP; 400.5–20 cm) (Fig. 2b). We analyzed 14 sediment samples from this core spanning depths 840.5–400.5 cm (Fig. 2b; Table 1).

3.2. Alkenone concentrations and distributions

Total alkenone concentrations were generally higher (i.e., 33 ± 51 μg/g C; average ± standard deviation) in the brackish portion of the Arkona Basin record than for the freshwater portion of the record (14 ± 21 μg/g C; Table 1). In the latter case, there were also sediment horizons that did not contain detectable concentrations of alkenones. In the sediments of the Yoldia Sea phase no alkenones were detected (Table 1). Fig. 3 shows some typical alkenone distributions from sediment core 318310. Alkenones are comprised of the more common $C_{37:2}$, $C_{37:3}$, and $C_{37:4}$ methyl (Me) ketones, $C_{38:2}$ and $C_{38:3}$ methyl (Me) and ethyl (Et) ketones, and the uncommon $C_{36:2}$ Me ketone. This latter alkenone has not

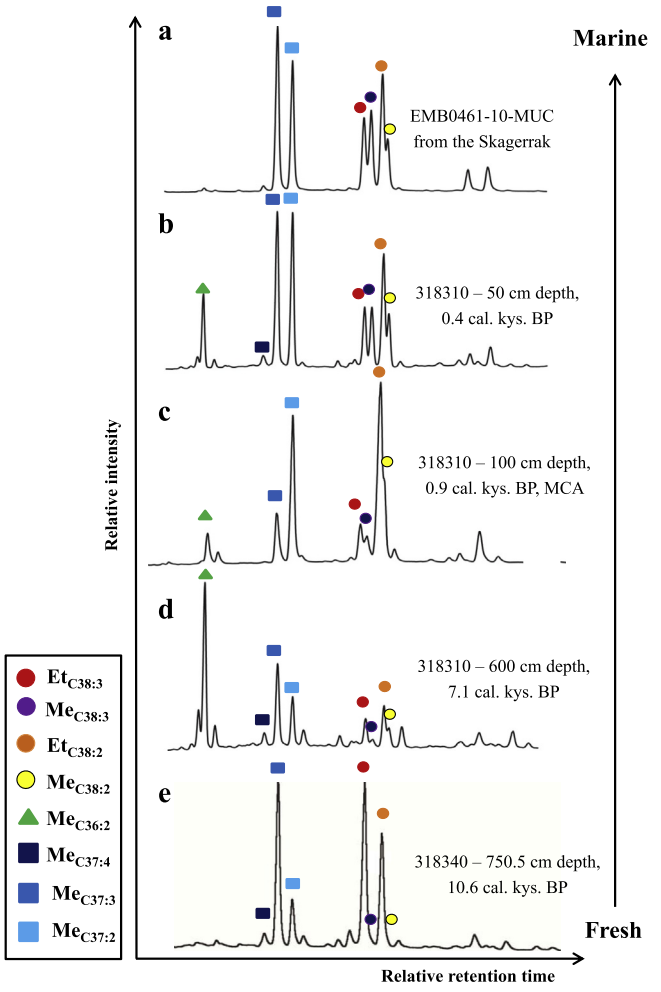

Fig. 3. Partial GC-FID chromatograms displaying alkenone distribution from various sediment horizons. (a) Sample EMB0461-10-MUC from the Skagerrak shows a typical marine distribution; (b) a sediment interval from 0.4 cal kyr BP (50 cm depth from core 318310) is from a brackish period and displays a distribution similar to the marine distribution except with the additional presence of the $C_{36:2}$ alkenone; (c) the sediment interval from 0.9 cal kyr BP (100 cm depth from core 318310) has a different distribution from the other depths in both cores with no $C_{37:4}$ alkenone, $C_{37:3} < C_{37:2}$, and a lower contribution of the $C_{36:2}$ alkenone relative to the C_{37} alkenones; (d) the sediment interval from 7.1 cal kyr BP (600 cm depth from core 318310) is from the period immediately following the Ancylus Lake/Littorina Sea transition and has an alkenone distribution characteristic of lower salinity haptophytes. Note the high relative abundance of the $C_{36:2}$ alkenone at this time; (e) the sediment interval from 750 cm from core 318340 representing the first part of the Ancylus Lake phase. Note that only traces of the $C_{36:2}$ alkenones are present and that the C_{38} ethyl ketones dominate the methyl ketones. The alkenones are color coded according to the legend with circles designating the C_{38} alkenones, triangles signifying the $C_{36:2}$ alkenone, and squares indicating the C_{37} alkenones. (For interpretation of the references to colour in this figure legend, the reader is referred to the web version of this article.)

been previously reported in sediments of the Baltic Sea. It is especially relatively abundant in sediments deposited during the Littorina Sea period. Skagerrak surface sediments (Fig. 1) were analyzed as a marine end member for comparison with the results obtained from the Arkona Basin record. We did not detect the presence of the $C_{36:2}$ alkenone in the Skagerrak sediments (Fig. 3a; Table 1). In sediment core 318310 a large difference in the relative abundance of C_{36}, C_{37} and C_{38} alkenones is observed from 600 cm

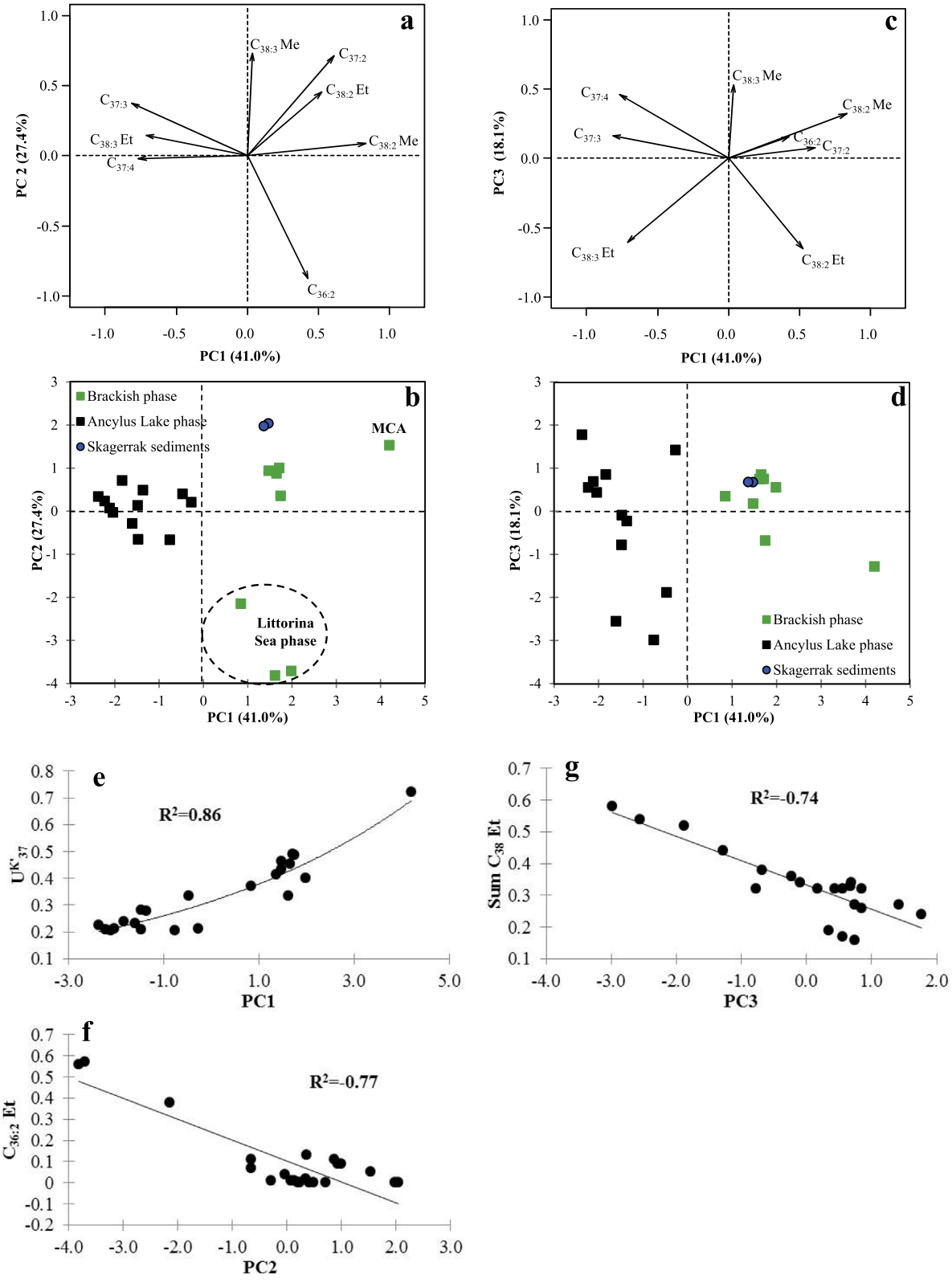

Fig. 4. Principal component analysis based on the standardized fractional abundances of the eight alkenones found consistently in the sediments from the Baltic Sea used in this study. Samples where alkenones were not detected were left out of the PCA. (a) Plot showing the scores of the alkenones and scores of the different sites on PC1 (41.0%) and PC2 (25.6%); (b) scores of the alkenones on PC1 and PC3 (18.1%) as well as the scores of the different sites. Scatter plots displaying the correlation of: (c) PC1 with $U^{K'}_{37}$ (R^2 = 0.86); (d) negative correlation of PC2 and $C_{36:2}$ Et (R^2 = 0.77); and (e) negative correlation with PC3 and the sum of the C_{38} Et (R^2 = 0.74).

depth (ca. 7.1 cal kyr BP; Fig. 3d), which is close to the Ancylus Lake/Littorina Sea transitional phase, to more recent sediments from the brackish phase of the Baltic Sea, i.e., at 100 cm (0.9 cal kyr, BP) and 50 cm (0.4 cal kyr BP) depth (Fig. 3b and c). For the Skagerrak surface sediments, the alkenone distribution is representative of a more open ocean setting (Fig. 3a). The alkenone distribution at 50 cm depth (Fig. 3b) is more similar to that of the Skagerrak sample than any of the other alkenone distributions shown (Fig. 3d), however, there are still a few differences between the two, such as the absence of the $C_{36:2}$ alkenone and the lower relative abundance of $C_{37:4}$ Me in the Skagerrak sediments.

For a statistical evaluation of alkenone distribution changes, PCA was performed on the distributions of C_{36}, C_{37} and C_{38} alkenones in the different sediments studied. Most of the variation is explained by principal component 1 (PC1; expressing 41% of the variance), which is related to the degree of unsaturation of the

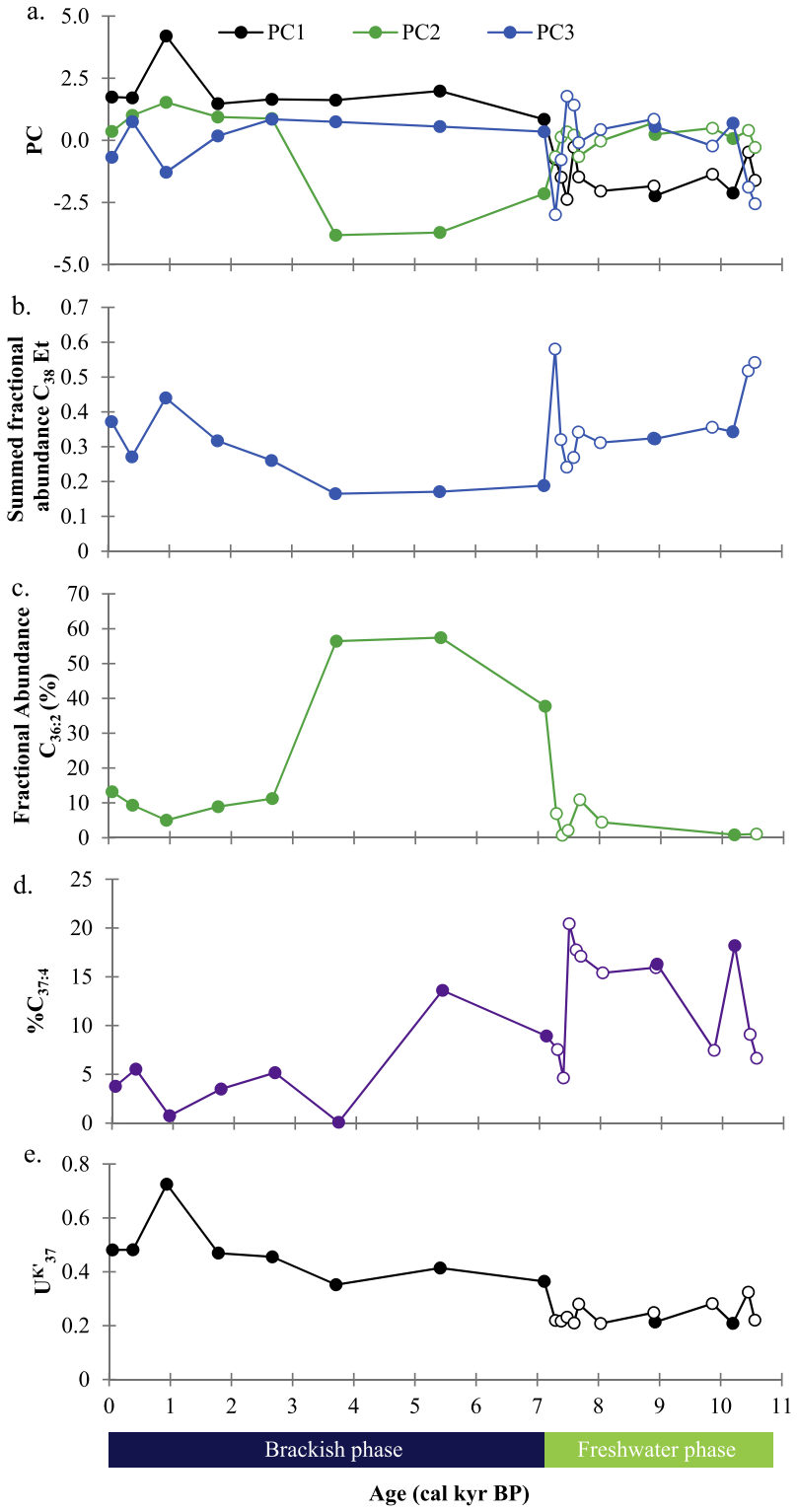

Fig. 5. Plots of the combined Arkona Basin record (sediment core 318310 designated by closed symbols and 318340 by open symbols) with age (cal kyr BP) for: (a) PC1–PC3; (b) summed fractional abundance of the C_{38} Et alkenones; (c) fractional abundance of the $C_{36:2}$ alkenone (%); (d) $\%C_{37:4}$; and (e) $U^{K'}_{37}$.

Table 2
Alkenone fractional abundances and alkenone based indices as well as the δD values of alkenones used in this study to examine salinity changes in the Baltic Sea sediments through time.

Site	Depth (cm)	Phase[a]	%$C_{37:4}$	Summed fractional abundance C_{38} Et alkenones	$U^{K'}_{37}$	δD $C_{36:2}$ alkenones	δD C_{37} alkenones	δD C_{38} alkenones
Skagerrak (EMB0461-10)	0–1		1.9	0.3	0.44	n.a.	−175.6	−184.2
Skagerrak (EMB0461-20)	0–1		1.8	0.3	0.41	n.a.	−174.9	−183.7
Arkona (core 318310)	20	PL/MB	3.8	0.4	0.48	−173.4	−207.5	−216.8
	50	PL/MB	5.5	0.3	0.48	n.d.	n.d.	n.d.
	100	PL/MB (MCA)	0.7	0.4	0.72	n.a.	−214.5	−220.5
	200	PL/MB	3.5	0.3	0.47	−166.1	−207.4	−216.4
	300	PL/MB	5.2	0.3	0.46	−169	−205.4	−209.2
	400	LS	0.1	0.2	0.35	n.d.	n.d.	n.d.
	500	LS	13.6	0.2	0.41	n.d.	n.d.	n.d.
	600	LS	8.9	0.2	0.36	−182.4	−168.7	−170.3
	625	AL	16.3	0.3	0.21	n.d.	n.d.	n.d.
	642.5	AL	18.2	0.3	0.21	n.d.	n.d.	n.d.
Arkona (core 318340)	400.5	AL/LS TP	7.5	0.6	0.22	n.d.	n.d.	n.d.
	420.5	AL/LS TP	4.6	0.3	0.22	n.d.	n.d.	n.d.
	440.5	AL/LS TP	20.4	0.2	0.23	n.d.	n.d.	n.d.
	464.5	AL/LS TP	17.8	0.3	0.21	n.d.	n.d.	n.d.
	480.5	AL/LS TP	17.1	0.3	0.28	n.d.	n.d.	n.d.
	500.5	AL	15.4	0.3	0.21	n.d.	n.d.	n.d.
	540.5	AL	15.9	0.3	0.25	n.d.	n.d.	n.d.
	584.5	AL	7.5	0.4	0.28	n.d.	n.d.	n.d.
	705.5	AL	9.1	0.5	0.32	n.d.	n.d.	n.d.
	750.5	AL	6.7	0.5	0.22	n.d.	n.d.	n.d.

[a] PL/MB = post Littorina/modern Baltic, MCA = Medieval Climate Anamoly, LS = Littorina Sea, TP = transitional phase, AL = Ancylus Lake.

alkenones with the most unsaturated alkenones scoring negatively on PC1 (Fig. 4a). This is confirmed by the good correlation ($r^2 = 0.86$) of the score on PC1 with $U^{K'}_{37}$ (Fig. 4e). The variation in PC2 (27%) appears to be mostly explained by the fractional abundance of the $C_{36:2}$ alkenone, which scores negatively on PC2 (Fig. 4a). Indeed, the score on PC2 significantly ($r^2 = 0.77$) negatively correlates with the fractional abundance of the $C_{36:2}$ alkenone (Fig. 4f). PC3 explains 18% of the variance with the C_{38} Et ketones scoring negatively on PC3 (Fig. 4c). PC3 correlates significantly ($r^2 = 0.77$) negatively with the summed fractional abundance of the $C_{38:3}$ and $C_{38:2}$ Et ketones (Fig. 4g).

Most sediments score between −1 and +1 on PC2, however, the Skagerrak sediments plot more positively (ca. 2.0) and sediments from the core 318310 from the Littorina Sea phase (sediment core depths 400, 500 and 600 cm) plot more negatively on PC2 (ca. −3.2) (Fig. 4b). Fig. 5a shows the scores of PC1-3 plotted as a function of age. This reveals that the score on PC1 is mostly negative for sediments older than 7.2 cal kyr BP and is mostly positive during the more recent phases of the Baltic Sea (younger than 7.2 cal kyr BP) (Fig. 5a). The score on PC2 consistently plots positively throughout the combined record from the Arkona Basin except for the sediment depths that correspond to the Littorina Sea phase (sediment core depths 400–600 cm from core 318310, which spans 7.1–3.7 cal kyr BP) and the end of the Ancylus Lake phase (sediment core depth 400.5 cm in core 318340, which spans 7.1–3.7 cal kyr BP; Fig. 5a and b). Two other core 318340 samples that plot slightly negatively for PC2 are depths 480.5 cm (7.7 cal kyr BP) and 750.5 cm (10.6 cal kyr BP) (Fig. 5a). PC3 scores mostly between −1 and 1 throughout the sediment record and for the Skagerrak samples, however, some samples that fall within the Ancylus Lake phase plot outside of this range as does sediment sample 100 cm from record 318310 (0.9 cal kyr BP; Figs. 4d and 5a).

3.3. δD of alkenones

We also determined δD values of alkenones on a subset of the samples from sediment core 318310 (Table 2), which can be an indicator of environmental conditions, mainly salinity and potentially haptophyte species composition (Schouten et al., 2005; van der Meer et al., 2008, 2015; Chivall et al., 2014; M'boule et al., 2014). The surface sediment samples from the Skagerrak have similar δD values for the C_{37} and C_{38} alkenones that fall between −175‰ and −185‰ (Fig. 6; Table 2). In the Arkona Basin the C_{37} and C_{38} alkenones have lower δD values during the more recent brackish phase going back to about 2.7 cal kyr BP, (−212.2 ± 5.5‰) (Fig. 6; Table 2). However, at the base of the Littorina Sea phase (7.1 cal kyr BP, 600 cm sediment depth from

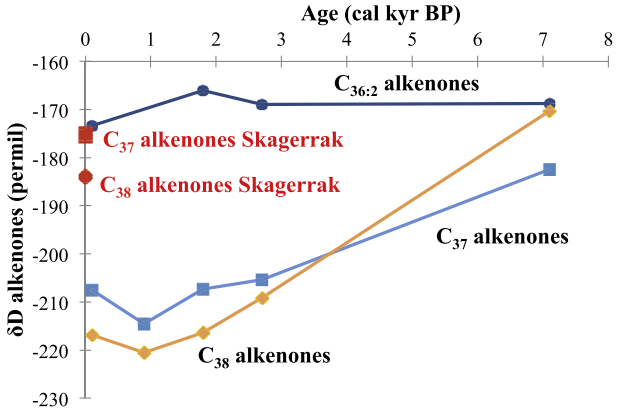

Fig. 6. δD values of the $C_{36:2}$, C_{37} and C_{38} alkenones plotted against age (cal kyr BP) from the record 318310 and the two Skagerrak surface sediment samples. In the Arkona Basin conditions were fresh until 7.8 cal kyr BP and brackish from 7.1 cal kyr BP onwards. The red squares designate the C_{37} alkenones and the red diamonds represent the C_{38} alkenones from the Skagerrak surface sediments. From the Arkona Basin sediment record (core 318310) dark blue circles denote the δD of the $C_{36:2}$ alkenones, the light blue squares signify the δD values C_{37} alkenones and the gold diamonds represent the δD of the C_{38} alkenones. (For interpretation of the references to colour in this figure legend, the reader is referred to the web version of this article.)

sediment core 318310), the δD values for C_{37} (−182.4‰) and C_{38} alkenones (−170.3‰) are much higher and, in contrast to the other samples, the C_{37} are more depleted in D than the C_{38} alkenones. The obtained δD values of the $C_{36:2}$ alkenone deposited during the brackish portion of the record in the Arkona Basin are enriched in D relative to the C_{37} and C_{38} alkenones from the same samples, but similar to those of the C_{37} and C_{38} alkenones encountered in the modern day Skagerrak (−169.3 ± 3.0‰). Just after the Ancylus Lake/Littorina Sea transition, the δD values of the $C_{36:2}$ alkenone (−168.7‰) is similar to that of the C_{38} alkenones (−170.3‰; Fig. 6; Table 2).

4. Discussion

4.1. Changes in sources of alkenones and its relation to changes in salinity

The observed changes in the relative abundances of the different alkenones through time may be a direct response of alkenone biosynthesis to changing environmental conditions of the Baltic Sea over the Holocene, or alternatively, the changing conditions could result in changing species composition leading to different alkenone distributions. There are many characteristics of alkenones that have been linked to haptophyte species composition and/or environmental conditions. The most important are:

(i) The degree of unsaturation of alkenones is commonly interpreted to be predominantly dependent on growth temperature (Brassell et al., 1986; Prahl and Wakeham, 1987).
(ii) The relative abundance of the $C_{37:4}$ alkenone is generally higher in coastal haptophytes that thrive at lower salinities and this predominance is even more extreme in freshwater systems (Rosell-Melé, 1998; Schulz et al., 2000; Blanz et al., 2005; Liu et al., 2008, 2011).
(iii) The ratio of C_{37}/C_{38} alkenones might be indicative of haptophyte species since different C_{37}/C_{38} values were observed for different haptophytes with coastal haptophytes generally showing higher ratios compared to more open ocean species (Prahl et al., 1988; Conte et al., 1998; Schulz et al., 2000). However, it has also been shown that environmental conditions, such as temperature, also affect the C_{37}/C_{38} ratio (Conte et al., 1998; Sun et al., 2007).
(iv) The presence of the uncommon $C_{36:2}$ alkenone, which has only been reported in the Black Sea (Xu et al., 2001; Prahl et al., 2006), Japan Sea (Fujine et al., 2006) and in an estuary in Florida (Van Soelen et al., 2014). Previous studies suggested it to be an indicator of brackish conditions (Xu et al., 2001; Fujine et al., 2006) and more recently, Coolen et al. (2009) proposed its biological origin in the Black Sea is likely to be a strain of low salinity-adapted *E. huxleyi*.
(v) The δD of alkenones are characteristic of certain types of haptophytes, but can also change with changing environmental conditions. Coastal haptophytes tend to isotopically fractionate less than more open marine haptophytes (Schouten et al., 2005; Chivall et al., 2014; M'boule et al., 2014), therefore, δD values can aid in assigning biological sources of sedimentary alkenones. However, hydrogen isotope fractionation also depends on environmental factors such as salinity, light intensity and growth rate (Schouten et al., 2005; Prahl et al., 2006; van der Meer et al., 2008, 2015; Wolhowe et al., 2015).

Some of these parameters were used to assign potential biological sources of the Baltic Sea sedimentary alkenones. To this end, the Arkona Basin data were compared with those from surface sediments of the Skagerrak (Figs. 4 and 6). Marine haptophytes, such as *E. huxleyi*, living at higher salinities and in more open ocean settings (like the Skagerrak; Egge et al., 2015) with a salinity of approximately 34 ppt (Danielssen et al., 1996) will fractionate at approximately 190‰ against D. Using a δD of Skagerrak water of ca. 0‰ (Fröhlich et al., 1988) the δD values for the C_{37} and C_{38} alkenones are predicted to be ca. −190‰ (Englebrecht and Sachs, 2005; Schouten et al., 2005; M'boule et al., 2014). The δD value of the C_{37} and C_{38} alkenones in the Skagerrak surface sediments is −180 ± 5‰ (Fig. 6; Table 2), indicating the haptophyte species in this region are predominantly of the marine type, most likely derived from *E. huxleyi*.

The alkenones in the sedimentary record of the Arkona Basin up to ca. 2.7 cal kyr BP have a distribution that is quite similar to that observed in Skagerrak surface sediments (Fig. 3a–c), which is typical of a marine haptophyte such as *E. huxleyi*. The low $\%C_{37:4}$ during this time (3.1 ± 2.3%) would also suggest that these alkenones are derived from marine type haptophytes (i.e., *E. huxleyi*) (Fig. 5d). However, the C_{37} and C_{38} alkenones have substantially lower δD values (−212 ± 6‰) than found in the Skagerrak surface sediments for the alkenones (−180 ± 5‰; Fig. 6; Table 2). There are two main factors to consider. Firstly, the present-day δD of surface waters in the Arkona Basin is ca. −40‰ averaged over the photic zone (Fröhlich et al., 1988), i.e., 40‰ depleted relative to the Skagerrak waters. This will shift the δD values of alkenones to substantially lower values (e.g., Englebrecht and Sachs, 2005). Secondly, culture studies have shown that hydrogen isotope fractionation is dependent on salinity, among other factors, with increased fractionation at lower salinities (e.g., M'boule et al., 2014). The present-day salinity of surface waters of the Arkona Basin is ~10 ppt (ICES-CIEM). If *E. huxleyi* would be able to grow at these low salinities, the alkenone δD value is estimated at ca. −270‰, which is substantially lower than the measured values for the C_{37} and C_{38} alkenones (−212 ± 6‰). This value was arrived upon by extrapolating the isotope fractionation (α)–salinity relationship to these low salinities (M'boule et al., 2014), and using the δD value for surface waters of −40‰ over the photic zone (Fröhlich et al., 1988). Consequently, this indicates that an *E. huxleyi* only origin for the C_{37} and C_{38} alkenones in the sedimentary record of the Arkona basin up to ca. 2.7 cal kyr BP, is unlikely. Haptophyte species adapted to lower salinities, such as *I. galbana* or *C. lamellosa*, fractionate less against D (Chivall et al., 2014; M'boule et al., 2014), and the alkenones produced will have a less negative δD value. For *I. galbana* (M'boule et al., 2014) a δD value of alkenones of ca. −180‰ can be estimated using a salinity of 10 ppt and a δD of surface waters of −40‰. This value is higher than the values observed for the C_{37} and C_{38} alkenones in the Arkona Basin up to ca. 2.7 cal kyr BP (i.e., between −205‰ and −220‰). This suggests that these sedimentary alkenones represent a mixture of alkenones produced by low salinity adapted haptophytes such as *I. galbana* and higher salinity adapted haptophytes such as *E. huxleyi*, with a more substantial contribution from the low salinity adapted haptophytes.

The $C_{36:2}$ alkenone was detected in the Arkona Basin sediments, but not in the Skagerrak surface sediments (Fig. 3; Table 1). This supports the premise that the $C_{36:2}$ alkenone is exclusively produced by a low-salinity adapted haptophyte (Coolen et al., 2009). PCA revealed that the fractional abundance of the $C_{36:2}$ alkenone is an important factor in the changing alkenone distributions in the Baltic Sea (Fig. 4a and f); i.e., PC2, explaining 27% of the total variance, is predominantly determined by the fractional abundance of the $C_{36:2}$ alkenone (Fig. 4a). In the sedimentary record of the Arkona Basin up to ca. 2.7 cal kyr BP, the fractional abundance of the $C_{36:2}$ alkenone amounts to 0.10 ± 0.03 (Fig. 5c; Table 1). From 7.1–3.7 cal kyr BP in the sediment record the fractional abundance of the $C_{36:2}$ alkenone increases to 0.51 ± 0.11 and it dominates the alkenone distribution (Figs. 3d and 5c;

Table 1). For the entire period of 7.1–0.1 cal kyr BP the δD values for the $C_{36:2}$ alkenone show only minor variation and are similar to the δD values for the C_{37} and C_{38} alkenones from the modern day Skagerrak (−170 ± 3‰; Fig. 6; Table 2). However, for most of the record the δD value of the $C_{36:2}$ alkenone is significantly higher than those of the C_{37} and C_{38} alkenones. Since the δD value of the $C_{36:2}$ alkenone is close to that (−180‰) calculated for *I. galbana* using a salinity of 10 ppt and a δD of surface waters of −40‰ (see above), this suggests that it is derived from a single low-salinity adapted haptophyte species. Previous studies (Coolen et al., 2009; Van Soelen et al., 2014) have also reported a substantial offset in δD values for C_{37} and $C_{36:2}$ alkenones with that of the $C_{36:2}$ alkenone being significantly higher. Van Soelen et al. (2014) concluded that the offset in δD values for C_{37} and $C_{36:2}$ alkenones found in an estuary in Florida is evidence that different haptophytes, yet still unknown, are producing the $C_{36:2}$ alkenone. Interestingly, close to the Ancylus Lake/Littorina Sea transition (7.1 cal kyr BP, 600 cm sediment depth from core 318310), which falls within the period characterized by the high fractional abundance of the $C_{36:2}$ alkenone, the δD values for C_{37} (−182.4‰) and C_{38} (−170.3‰) alkenones are much higher than in the other Arkona Basin samples and similar to the δD values of the $C_{36:2}$ alkenone (Fig. 6; Table 2). This suggests a similar origin for most of the C_{36}, C_{37} and C_{38} alkenones at this time, most likely a low salinity adapted haptophyte species. This is strongly supported by the deviating alkenone distribution at this time (Fig. 3d) dominated by the $C_{36:2}$ alkenone. The observed trends in δD values of alkenones over the period between 7.1 and 0.1 cal kyr BP, thus, corroborate the idea that during this period in the Baltic Sea there is more than one alkenone producing haptophyte species.

From ~7.1–3.7 cal kyr BP, during the Littorina Sea phase in the Baltic Sea, the $C_{36:2}$ ratio is highest demonstrating the greatest contribution from these low-salinity adapted haptophytes and the $\%C_{37:4}$ is more variable during this period ranging from 0.1–13.6%. This suggests mutable input from non-marine type haptophytes and therefore potentially fluctuating salinities (Fig. 5d; Table 2). The enrichment in the δD of the C_{37} and C_{38} alkenones corroborates the contribution from non-marine haptophytes as well (Fig. 6). Why the $\%C_{37:4}$ and the fractional abundance of the $C_{36:2}$ alkenone is higher and the C_{37} and C_{38} alkenones are more enriched in D during the Littorina Sea phase than after is not clear since they are both brackish water periods. Possibly this is related to the period after the Ancylus Lake/Littorina Sea transition being a time of not only low, but also variable salinity. Perhaps the haptophytes producing the $C_{36:2}$ alkenone had a competitive advantage over other haptophytes at this time because they were better adapted to changing salinities, or alternatively, certain haptophyte species biosynthesize this compound in response to changing salinities or marine haptophytes brought in from the North Sea were not yet established. These possibilities suggest that variable salinity was a characteristic of the Littorina Sea phase.

Prior to 7.1 cal kyr BP in the Arkona Basin sediment record we do not have δD values of alkenones to report, however, some remarkable changes in the alkenone distributions are observed. Firstly, the $U^{K'}_{37}$ is lower prior to the Ancylus Lake/Littorina Sea transition (Fig. 5e) potentially due to a change in the composition of the haptophyte community as indicated by the somewhat higher fractional abundance of the $C_{37:4}$ at this time (Fig. 5d; Table 1). Secondly, the fractional abundance of the $C_{36:2}$ alkenone is relatively low from 10.7 cal kyr BP up to the transition (0.02 ± 0.03; Fig. 5c; Table 1). Thirdly, during the transitional phases of this time period, both the Yoldia Sea phase to Ancylus Lake transition (ca. 10.7–10.6 cal kyr BP) and at the Ancylus Lake/Littorina Sea transition (ca. 7.3 cal kyr BP), the alkenone distributions are dominated by C_{38} ethyl alkenones (i.e., a low score on PC3; Fig. 4c and d and a summed average fractional abundance of 0.55 ± 0.03; Fig. 5b; Table 1). The lower fractional abundance of the $C_{36:2}$ alkenone during the Ancylus Lake phase, (Fig. 5c; Table 1) suggests that most likely a change in haptophyte species composition occurred related to salinity. Additionally, the $C_{36:2}$ alkenone is absent in the Arkona Basin sedimentary record from 10.2–8.0 cal kyr BP (Fig. 5c; Table 1). Since it is a potential indicator for the low salinity-adapted species, but not freshwater haptophyte species, the presence of the $C_{36:2}$ alkenone prior to the Anyclus Lake phase ending suggests marine influxes had already begun in the basin at that time. A diatom study by Witkowski et al. (2005) reported that the first brackish water inflows began just before this time period, i.e., between 8.9 and 8.4 cal kyr BP. The presence of the $C_{36:2}$ alkenone from 10.6–10.2 cal kyr BP aligns with the ending of the slightly brackish Yoldia Sea phase. Lastly, the higher $\%C_{37:4}$ during the Ancylus Lake phase verifies that there was an increase in freshwater haptophytes during this time.

4.2. Comparison with the Holocene alkenone record of the Black Sea

A previous study of alkenones in the Black Sea (Coolen et al., 2009) reported similar trends with respect to the fractional abundance of the $C_{36:2}$ alkenone to those reported here for the Baltic Sea. The Black Sea experienced a somewhat comparable geological history to the Baltic Sea. In the early Holocene it was a freshwater lake until a connection was established with the Aegean and Mediterranean Seas due to the global transgression allowing the influx of more saline waters (Ryan et al., 1997). The permanent establishment of this connection is dated at ca. 7.2 cal kyr BP (Ryan et al., 1997; Ballard et al., 2000). The resultant increase in salinity is reflected by the sedimentary sequence revealing a transition from banded clay with graded sand and silt layers (Unit III) to sapropel mud (Unit II) (Ross et al., 1970). As the influx of salty Mediterranean waters continued it caused an increase in the surface salinity of the Black Sea allowing a massive growth of *E. huxleyi* (Jones and Gagnon, 1994) in the basin ca. 2.7 cal kyr BP, resulting in deposition of a coccolith ooze (Jones and Gagnon, 1994). The abundance in *E. huxleyi* at this time has been attributed to a surface water salinity increasing above 11 ppt and the base of Unit I is generally defined as the horizon that reveals the first invasion of *E. huxleyi*, ca. 700 yr earlier (Fig. 7) (Hay, 1988; Arthur and Dean, 1998).

Since the salinity changes in the Baltic Sea and Black Sea occurred around the same time (~7.2 cal kyr BP), we compared the relative abundance of the $C_{36:2}$ alkenone from the Baltic Sea directly to that in the Black Sea reported by Coolen et al. (2009) (Fig. 7a). In both the Baltic Sea and Black Sea the fractional abundance of the $C_{36:2}$ alkenone is rapidly increasing to values of 40–70% just after the inflow of more saline waters started. Subsequently, a period of sustained high fractional abundances follows in both basins up to ca. 2.6 cal kyr BP. The higher resolution record of the Black Sea shows that the period between 7.0 and 5.4 cal kyr BP is characterized by the highest values (up to 75%), followed by a drop to a fractional abundance of ca. 25% for the period 5.0–2.6 cal kyr BP. This latter period is interrupted by the horizon of the first invasion of *E. huxleyi* at 3.5 cal kyr BP when the fractional abundance drops to 5%. For the Baltic Sea the fractional abundance of the $C_{36:2}$ alkenone is high throughout the 7.0–2.6 cal kyr BP period although this is based on a small dataset. In both basins the fractional abundance of the $C_{36:2}$ alkenone is substantially reduced in the most recent period (2.6–0.0 cal kyr BP) although for the Baltic Sea it does not drop to the low values seen in the Black Sea (i.e., 1%) and it increases toward the present day situation (Fig. 7a). In conclusion, we note a quite similar behavior for the fractional abundance of the $C_{36:2}$ alkenone in both enclosed basins with limited connection to the open ocean. This may relate to a

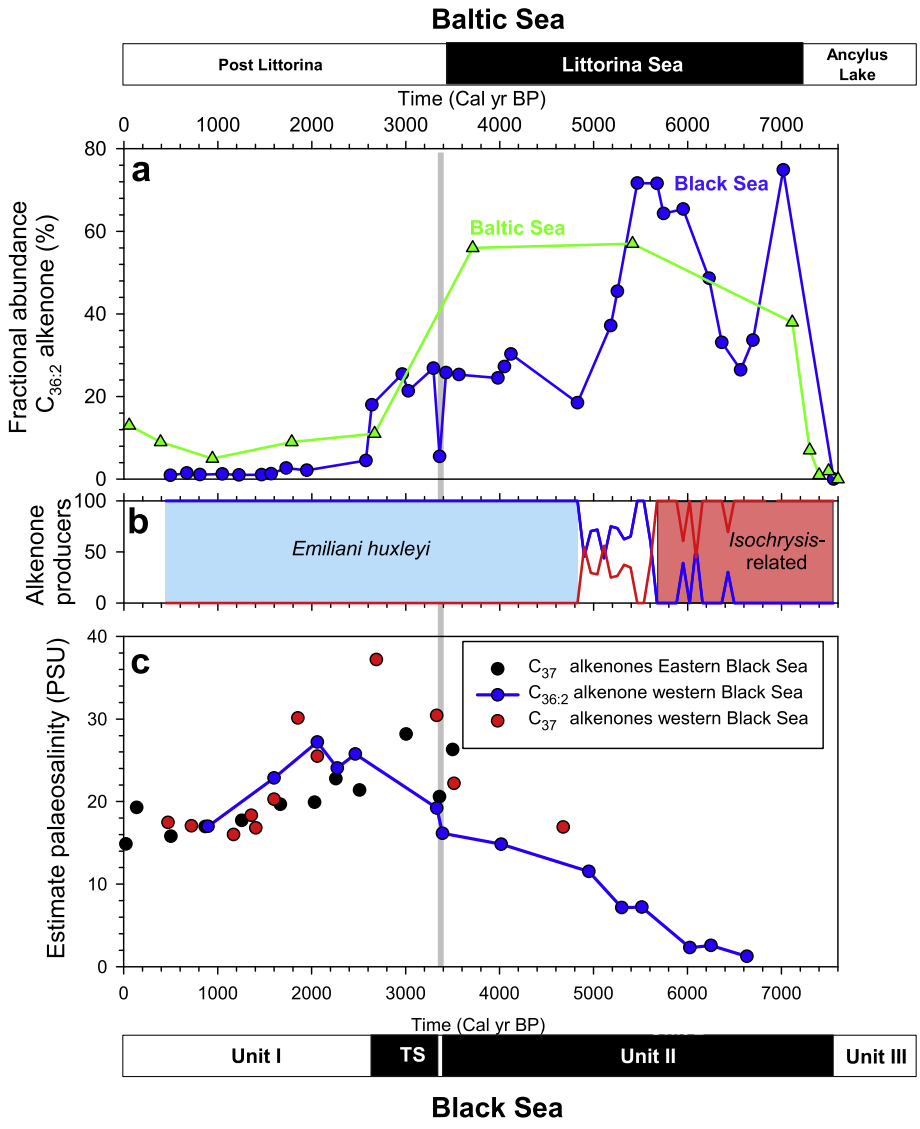

Fig. 7. Comparison of $C_{36:2}$ alkenone abundance data for the Baltic Sea and the Black Sea over the Holocene. Top panel (a) shows the fractional abundance of the $C_{36:2}$ alkenone relative to the C_{36}–C_{38} alkenones for the Black Sea (blue circles; data from Coolen et al., 2009) and Baltic Sea (green triangles; this study). The middle panel (b) shows the haptophyte community composition in the Black Sea as reconstructed based on DGGE analysis of partial 18S rRNA genes amplified with a specific haptophyte primer set with *Isochrysis*-related haptophytes in red and *E. huxleyi* in blue (data modified from Coolen et al., 2009; note that in their Fig. 3 relative abundance data is shown based on the relative abundance of all DGGE bands not only those related to alkenone-producing haptophytes; Coolen, personal communication). These data are in agreement with earlier haptophyte 18S rRNA gene work on a box core just penetrating Unit 2 from a deep water site in the eastern Black Sea (Coolen et al., 2006). The bottom panel (c) shows reconstructed salinities for the Black Sea based on the hydrogen isotopic compositions of the $C_{36:2}$ and C_{37} alkenones. For all data the fractionation factor α was calculated using a water hydrogen isotopic composition of −20‰ (Swart, 1991). Salinities were reconstructed based on the α-salinity relationship for *Isochrysis galbana* ($\alpha = 0.0019 \times S + 0.836$; M'boule et al., 2014) for the $C_{36:2}$ alkenone and *E. huxleyi* ($\alpha = 0.0021 \times S + 0.740$; M'boule et al., 2014) for the C_{37} alkenones. Original alkenone hydrogen isotope data are for the eastern Black Sea from van der Meer et al. (2008) and for the western Black Sea from Giosan et al. (2012). The stratigraphy for the Baltic Sea (top) and Black Sea (bottom) is indicated. TS denotes transition sapropel. Note that the stratigraphy described for the Black Sea core in the study of Coolen et al. (2009) and Giosan et al. (2012) has been adjusted to fit the commonly applied stratigraphy for the Black Sea (see lowermost part of the figure), i.e., the layer of the first invasion of *E. huxleyi* (gray bar in the other panels) is taken as the start of Unit 1 deposition (Hay, 1988; Arthur et al., 1994; Jones and Gagnon, 1994). In the sediment core used in the work of Coolen et al. (2009) this layer is not clearly revealed by an increase of the carbonate content, but the alkenone distribution shows a distinct change at ca. 3350 cal yr BP (see sudden decrease of the relative abundance of the $C_{36:2}$ alkenone in panel a; in addition this horizon is also characterized by a 3–4-fold increase in total alkenone concentration and the detection of C_{39} alkenones; Coolen et al., 2009) toward a composition highly comparable to the upper part of Unit I that is composed of coccolith ooze. Their reported radiocarbon date for this section (3,360 ± 68 cal yr BP) is by this adjustment in good agreement with the reported age of the base of Unit I at other locations in the Black Sea (Hay, 1988; Arthur et al., 1994; Jones and Gagnon, 1994). (For interpretation of the references to colour in this figure legend, the reader is referred to the web version of this article.)

somewhat comparable response to the global sea level transgression during the Holocene. For the Black Sea substantial additional data is available for the interpretation of this trend and this may help, by analogy, to provide a more detailed interpretation of the Baltic Sea record.

Coolen et al. (2006, 2009) provided, through ancient DNA analysis, clues on the biological origin of the sedimentary alkenone in the Black Sea. The most extensive record comes from a site in the western Black Sea. It reveals that during deposition of the base of Unit II *Isochrysis*-related haptophytes thrived (Fig. 7c). This fits with the time of the newly established connection with the Mediterranean since these types of haptophytes are adapted to low salinity. Subsequently, there is a short period (5.7–4.8 cal kyr BP) where Coolen et al. (2009) detected both *Isochrysis*-related haptophytes and *E. huxleyi*, followed by a period where only ancient DNA of *E. huxleyi* was found. When this information is

combined with the record of the fractional abundance of the $C_{36:2}$ alkenone (Fig. 7a), it is evident that this alkenone must have been produced by *Isochrysis*-related haptophytes since the period of highest fractional abundance (up to 75%) falls in the period where only ancient DNA of *Isochrysis*-related haptophytes is detected (Fig. 7). However, the $C_{36:2}$ alkenone also occurs (albeit at a substantially reduced fractional abundance) in more recent periods when only ancient DNA of *E. huxleyi* is detected, suggesting that this haptophyte may also produce this alkenone. However, this latter conclusion is at odds with the large difference (90–100‰) in δD composition of the $C_{36:2}$ and C_{37} alkenones as reported by Giosan et al. (2012) for this section, which indicates clearly distinct biological sources for these alkenones. In fact, when the δD record of the $C_{36:2}$ alkenone is combined with the recent determination of the isotopic fractionation factor α for *Isochrysis galbana* (M'boule et al., 2014) to estimate palaeosalinity of the surface waters of the Black Sea over the Holocene, we obtain a record (Fig. 7c; blue line) that is in good agreement with our general concept of the development of surface salinity of the Black Sea. In the lowermost part of Unit II the estimated palaeosalinity is only a few ppt, it subsequently rises to 15 ppt at the Unit I/II transition, reaches a maximum of ca. 26 ppt at 2.0 cal kyr BP and then declines to 17 ppt for the most recent period. These data are in good agreement with salinity calculations (Fig. 7c) based on δD data of C_{37} alkenones in cores from both the western and eastern Black Sea (van der Meer et al., 2008; Giosan et al., 2012) in combination with the isotopic fractionation factor α for *E. huxleyi* (M'boule et al., 2014). For the period where the fractional abundance of the $C_{36:2}$ alkenone is still elevated (i.e., up to 2.6 cal kyr BP) these estimations of paleosalinity are on the high end (except for the horizon reflecting the first invasion of *E. huxleyi* in the Eastern Basin). This is most likely caused by the fact that the $C_{36:2}$ alkenone-producing haptophytes are also contributing D-enriched C_{37} alkenones to the total pool of C_{37} alkenones, influencing the palaeosalinity calculation that is based on a 100% origin from *E. huxleyi*. Hence, the δD data of the $C_{36:2}$ alkenone in combination with the salinity calculations strongly suggest that the $C_{36:2}$ alkenone has been produced by an *Isochrysis*-related haptophyte and not by a lower salinity adapted strain of *E. huxleyi*, as suggested previously (Coolen et al., 2009). It remains unclear why ancient DNA of this haptophyte is only detected for the period 7.4–4.8 cal kyr BP. However, it is known that Denaturing Gradient Gel Electrophoresis (DGGE), the method used by Coolen et al. (2009) to detect ancient DNA is only able to quantify the predominant DNA sequences.

Combining the fractional abundance record of the $C_{36:2}$ alkenone (Fig. 7a) with the paleosalinity record (Fig. 7c) now makes it possible to determine the optimal salinity for the *Isochrysis*-related haptophyte producing the $C_{36:2}$ alkenone. In the Black Sea at salinities from 2–8 ppt, the $C_{36:2}$ alkenone dominates the alkenone distribution. At a salinity of up to ca. 19 ppt the $C_{36:2}$ alkenone can still contribute substantially (25%) and above this level it becomes a minor alkenone. It is clear that salinity is not the only environmental control on the $C_{36:2}$ alkenone-producing haptophyte since when in recent times salinities drop to ca. 17 ppt, the $C_{36:2}$ alkenone still remains a minor alkenone (Fig. 7).

The $C_{36:2}$ alkenone data of the Black Sea allow the interpretation of the $C_{36:2}$ alkenone record of the Baltic Sea in term of changes in salinity. This should be done cautiously since it is clear that other environmental factors also may have an effect. Nevertheless, the sudden increase of the fractional abundance of the $C_{36:2}$ alkenone record at the Ancylus Lake/Littorina Sea transition is highly comparable to what happened in the Black Sea at the Unit III/II transition and indicates an incursion of marine waters into the freshwater lakes most probably by the worldwide sea level transgression, resulting in a modest increase in surface water salinity to ca. 2 ppt. In the Baltic Sea the fractional abundance of the $C_{36:2}$ alkenone remains high until ca. 3.0 cal kyr BP, suggesting that the salinity of the surface waters of the Arkona Basin increased at a lower rate than in the Black Sea. The lowest fractional abundance of the $C_{36:2}$ alkenone is recorded in the Arkona Basin at 0.9 cal kyr BP, suggesting that the salinity was highest at that time, which corresponds to the medieval climate anomaly (MCA, which occurred between 950 and 1250 AD). This trend is similar to salinity records for the whole Baltic Sea based on combined proxies and modeling (Gustafsson and Westman, 2002) although the maximum salinity is thought to be earlier even when we correct for the different age models. Generally, it is believed that the Littorina phase of the Baltic Sea was more saline than the post-Littorina phase, however, other studies do not reveal this difference (Westman and Sohlenius, 1999; Andren et al., 2000; Andrén et al., 2002; Witkowski et al., 2005) or show the opposite (Emeis et al., 2003).

4.3. Potential uses of alkenones as environmental indicators for SST/LST

The indices and ratios we have presented in this study all corroborate that a haptophyte species composition change, most likely driven by a salinity shift, occurred during the Yoldia Regression (10.6 cal kyr BP), the Ancylus Lake/Littorina Sea transition (7.7–7.2 cal kyr BP), and at the MCA (0.9 cal kyr BP). The results also indicate that the haptophyte species composition since 7.2 cal kyr BP in the Baltic Sea basin is a combination of marine (*E. huxleyi* type) and low-salinity adapted haptophytes. This indicates that higher salinity conditions have prevailed since the Ancylus Lake/Littorina Sea transition.

To determine how shifts in haptophyte species composition in the Baltic Sea could affect paleoclimate reconstructions using long chain alkenones, we examined the $U^{K'}_{37}$ index over the Holocene. $U^{K'}_{37}$ values changed across the Ancylus Lake/Littorina Sea transition with lower values (0.24 ± 0.04) during the Ancylus Lake phase and an increase in the $U^{K'}_{37}$ index after 7.2 cal kyr BP (0.47 ± 0.12; Fig. 5e; Table 2). This resulted in an increase in average estimated SST/LST based on the $U^{K'}_{37}$ index from ~6 °C during the Ancylus Lake phase to ~13 °C during the brackish phase. We believe that variations in haptophyte community composition resulting from fluctuating salinity is most likely responsible for this change in $U^{K'}_{37}$ values and the corresponding unrealistic increase in SST/LST over the Ancylus Lake/Littorina Sea transition. The highest contribution of the $C_{36:2}$ alkenone occurred during the Littorina Sea phase, which indicates salinity was relatively low at that time. The presence of this alkenone even in the more recent phase of the Baltic Sea is evidence of the continued contribution from low salinity adapted haptophytes, which are most likely complicating the use of alkenone unsaturation ratios for SST reconstructions in this region. Schulz et al. (2000) demonstrated in a study performed in the Baltic Sea that $U^{K'}_{37}$ varied regionally depending on salinity and that higher salinity areas in the Baltic had higher $U^{K'}_{37}$ values and vice versa. Since previous studies have also shown that alkenone distributions co-vary not only with temperature changes, but also with salinity driven changes in haptophyte species composition (Coolen et al., 2004, 2009) we cannot apply the $U^{K'}_{37}$ index for SST/LST reconstructions in the Baltic Sea basin over the Holocene.

Interestingly, we observed that during the brackish phase the alkenone distribution at 0.9 cal kyr BP (100 cm depth) is unique compared to the other sediment samples (Fig. 3) from the brackish phase. This sediment horizon has the lowest contribution of the $C_{36:2}$ alkenone, the lowest $\%C_{37:4}$ and the highest fractional abundance of the C_{38} Et alkenone (Fig. 5b–d; Tables 1 and 2), all indicating the increased presence of marine type haptophyte species and therefore that more marine conditions prevailed in the Baltic Sea at

this time. This sample falls within the MCA, also known as the Medieval Warm Period. The lower contribution of the $C_{37:3}$ alkenone compared with $C_{37:2}$ corroborate that warmer temperatures (Fig. 3c) occurred during this time, although the minor contribution of *Isochrysis*-related haptophytes do not allow absolute SST determination.

5. Conclusions

This research demonstrates the usefulness of alkenone distributions along with the δD of the alkenones for paleosalinity studies in the Baltic Sea and other environments as well. Both alkenone distributions and hydrogen isotopic composition indicate a shift in haptophyte species composition in the Arkona Basin of the Baltic Sea from the Ancylus Lake to the Littorina Sea phase, ca. 7.2 cal kyr BP, from lacustrine to brackish type haptophytes, corresponding to the incursion of marine waters that occurred in the Baltic Sea at that time as a consequence of the global sea level rise. During the Littorina Sea Phase the fractional abundance of the $C_{36:2}$ alkenone remains high, suggesting that salinity did not rise above 8 ppt. From ca. 3.0 cal kyr BP onwards the fractional abundance of the $C_{36:2}$ alkenone is lower, suggesting a slightly higher salinity. During this phase there is a substantial offset in δD values with the $C_{36:2}$ alkenone substantially more enriched than the C_{37} alkenones. The presence of the $C_{36:2}$ alkenone in the Baltic Sea as well as the δD record suggest it is produced by a different species of haptophyte adapted to lower salinity conditions that is not contributing much to the production of C_{37} and C_{38} alkenones. The contribution of alkenones from lower salinity adapted species in the Baltic Sea hinders the use of the $U^{K'}_{37}$ index for SST reconstructions.

Acknowledgements

We thank M. Verweij for assistance with the GC analysis, A. Mets for help with the GC–MS analysis and two anonymous referees for helpful comments. This work was supported by the European Research Council under the European Union's Seventh Framework Programme (FP7/2007-2013) and ERC grant agreement 226600. MvdM was funded by the Dutch Organisation for Scientific Research (NWO) through a VIDI grant (864.09.011). JSSD receives funding from the Netherlands Earth System Science Center (NESSC) though a gravitation grant (024.002.001) from the Dutch Ministry for Education, Culture and Science.

Associate Editor—**Bart van Dongen**

References

Andren, E., Andrén, T., Sohlenius, G., 2000. The Holocene history of the southwestern Baltic Sea as reflected in a sediment core from the Bornholm Basin. Boreas 29, 233–250.

Andrén, T., Lindeberg, G., Andrén, E., 2002. Evidence of the final drainage of the Baltic Ice Lake and the brackish phase of the Yoldia Sea in glacial varves from the Baltic Sea. Boreas 31, 226–238.

Arthur, M.A., Dean, W.E., Neff, E.D., Hay, B.J., King, J., Jones, G., 1994. Varve calibrated records of carbonate and organic carbon accumulation over the last 2000 years in the Black Sea. Global Biogeochemical Cycles 8, 195–217.

Arthur, M.A., Dean, W.E., 1998. Organic-matter production and preservation and evolution of anoxia in the Holocene Black Sea. Paleoceanography 13, 395–411.

Ballard, R.D., Coleman, D.F., Rosenberg, G.D., 2000. Further evidence of abrupt Holocene drowning of the Black Sea shelf. Marine Geology 170, 253–261.

Björck, S., 1995. A review of the history of the Baltic Sea, 13.0–8.0 ka BP. Quaternary International 27, 19–40.

Blanz, T., Emeis, K.C., Siegel, H., 2005. Controls on alkenone unsaturation ratios along the salinity gradient between the open ocean and the Baltic Sea. Geochimica et Cosmochimica Acta 69, 3589–3600.

Brassell, S.C., Eglinton, G., Marlowe, I.T., Pflaumann, U., Sarnthein, M., 1986. Molecular stratigraphy: a new tool for climatic assessment. Nature 320, 129–133.

Chivall, D., M'Boule, D., Sinke-Schoen, D., Sinninghe Damsté, J.S., Schouten, S., van der Meer, M.T., 2014. Impact of salinity and growth phase on alkenone distributions in coastal haptophytes. Organic Geochemistry 67, 31–34.

Chu, G., Sun, Q., Li, S., Zheng, M., Jia, X., Lu, C., Liu, J., Liu, T., 2005. Long-chain alkenone distributions and temperature dependence in lacustrine surface sediments from China. Geochimica et Cosmochimica Acta 69, 4985–5003.

Conte, M.H., Thompson, A., Lesley, D., Harris, R.P., 1998. Genetic and physiological influences on the alkenone/alkenoate versus growth temperature relationship in *Emiliania huxleyi* and *Gephyrocapsa oceanica*. Geochimica et Cosmochimica Acta 62, 51–68.

Coolen, M.J., Muyzer, G., Rijpstra, W.I.C., Schouten, S., Volkman, J.K., Sinninghe Damsté, J.S., 2004. Combined DNA and lipid analyses of sediments reveal changes in Holocene haptophyte and diatom populations in an Antarctic lake. Earth and Planetary Science Letters 223, 225–239.

Coolen, M.J., Boere, A., Abbas, B., Baas, M., Wakeham, S.G., Sinninghe Damsté, J.S., 2006. Ancient DNA derived from alkenone-biosynthesizing haptophytes and other algae in Holocene sediments from the Black Sea. Paleoceanography 21. http://dx.doi.org/10.1029/2005PA001188.

Coolen, M.J., Saenz, J.P., Giosan, L., Trowbridge, N.Y., Dimitrov, P., Dimitrov, D., Eglinton, T.I., 2009. DNA and lipid molecular stratigraphic records of haptophyte succession in the Black Sea during the Holocene. Earth and Planetary Science Letters 284, 610–621.

Cranwell, P.A., 1985. Long-chain unsaturated ketones in recent lacustrine sediments. Geochimica et Cosmochimica Acta 49, 1545–1551.

D'Andrea, W.J., Lage, M., Martiny, J.B.H., Laatsch, A.D., Amaral-Zettler, L.A., Sogin, M. L., Huang, Y., 2006. Alkenone producers inferred from well-preserved 18S rDNA in Greenland lake sediments. Journal of Geophysical Research Biogeosciences 111. http://dx.doi.org/10.1029/2005JG000121.

Danielssen, D.S., Svendsen, E., Ostrowski, M., 1996. Long-term hydrographic variation in the Skagerrak based on the section Torungen-Hirtshals. ICES Journal of Marine Science 53, 917–925.

Dean Jr., W.E., 1974. Determination of carbonate and organic matter in calcareous sediments and sedimentary rocks by loss on ignition: comparison with other methods. Journal of Sedimentary Research 44, 242–248.

de Leeuw, J.W., van der Meer, F.W., Rijpstra, W.I.C., Schenck, P.A., 1980. On the occurrence and structural identification of long chain unsaturated ketones and hydrocarbons in sediments. Physics and Chemistry of the Earth 12, 211–217.

Dillon, J.T., Longo, W.M., Zhang, Y., Torozo, R., Huang, Y., 2016. Identification of double-bond positions in isomeric alkenones from a lacustrine haptophyte. Rapid Communications in Mass Spectrometry 30, 112–118.

Egge, E.S., Eikrem, W., Edvardsen, B., 2015. Deep-branching novel lineages and high diversity of Haptophytes in the Skagerrak (Norway) uncovered by 454 pyrosequencing. Journal of Eukaryotic Microbiology 62, 121–140.

Emeis, K.-C., Struck, U., Blanz, T., Kohly, A., Voβ, M., 2003. Salinity changes in the central Baltic Sea (NW Europe) over the last 10000 years. Holocene 13, 411–421.

Englebrecht, A.C., Sachs, J.P., 2005. Determination of sediment provenance at drift sites using hydrogen isotopes and unsaturation ratios in alkenones. Geochimica et Cosmochimica Acta 69, 4253–4265.

Fröhlich, K., Grabczak, J., Rozanski, K., 1988. Deuterium and oxygen-18 in the Baltic Sea. Chemical Geology 72, 77–83.

Fujine, K., Yamamoto, M., Tada, R., Kido, Y., 2006. A salinity-related occurrence of a novel alkenone and alkenoate in Late Pleistocene sediments from the Japan Sea. Organic Geochemistry 37, 1074–1084.

Giosan, L., Coolen, M.J., Kaplan, J.O., Constantinescu, S., Filip, F., Filipova-Marinova, M., Kettner, A.J., Thom, N., 2012. Early anthropogenic transformation of the Danube-Black Sea system. Scientific Reports 2, 582. http://dx.doi.org/10.1038/srep00582.

Gustafsson, B.G., Westman, P., 2002. On the causes for salinity variations in the Baltic Sea during the last 8500 years. Paleoceanography 17. http://dx.doi.org/10.1029/2000PA000572.

Hay, B.J., 1988. Sediment accumulation in the central western Black Sea over the past 5100 years. Paleoceanography 3, 491–508.

Hyvärinen, H., Donner, J., Kessel, H., Raukas, A., 1988. The Litorina and Limnaea Sea in the northern and central Baltic, in Problems of the Baltic Sea History. Annales Academiae Scientiarum Fennicae 148, 25–35.

Jensen, J.B., 1995. A Baltic Ice Lake transgression in the southwestern Baltic: evidence from Fakse Bugt, Denmark. Quaternary International 27, 59–68.

Jensen, J.B., Bennike, O., Witkowski, A., Lemke, W., Kuijpers, A., 1999. Early Holocene history of the southwestern Baltic Sea: the Ancylus Lake stage. Boreas 28, 437–453.

Jones, G.A., Gagnon, A.R., 1994. Radiocarbon chronology of Black Sea sediments. Deep Sea Research Part I: Oceanographic Research Papers 41, 531–557.

Leipe, T., Tauber, F., Vallius, H., Virtasalo, J., Uścinowicz, S., Kowalski, N., Hille, S., Lindgren, S., Myllyvirta, T., 2011. Particulate organic carbon (POC) in surface sediments of the Baltic Sea. Geo-Marine Letters 31, 175–188.

Liu, W., Liu, Z., Fu, M., An, Z., 2008. Distribution of the C_{37} tetra-unsaturated alkenone in Lake Qinghai, China: a potential lake salinity indicator. Geochimica et Cosmochimica Acta 72, 988–997.

Liu, W.G., Liu, Z.H., Wang, H.Y., He, Y.X., Wang, Z., Xu, L.M., 2011. Salinity control on long-chain alkenone distributions in lake surface waters and sediments of the northern Qinghai-Tibetan Plateau, China. Geochimica et Cosmochimica Acta 75, 1693–1703.

Longo, W.M., Theroux, S., Giblin, A.E., Zheng, Y., Dillon, J.T., Huang, Y., 2016. Temperature calibration and phylogenetically distinct distributions for

freshwater alkenones: evidence from northern Alaskan lakes. Geochimica et Cosmochimica Acta 180, 177–196.
Nakamura, H., Sawada, K., Araie, H., Suzuki, I., Shiraiwa, Y., 2014. Long chain alkenes, alkenones and alkenoates produced by the haptophyte alga *Chrysotila lamellosa* CCMP1307 isolated from a salt marsh. Organic Geochemistry 66, 90–97.
Nakamura, H., Sawada, K., Araie, H., Shiratori, T., Ishida, K.-I., Suzuki, I., Shiraiwa, Y., 2016. Composition of long chain alkenones and alkenoates as a function of growth temperature in marine haptophyte *Tisochrysis lutea*. Organic Geochemistry 99, 78–89.
Nelson, D.B., Sachs, J.P., 2014. The influence of salinity on D/H fractionation in alkenones from saline and hypersaline lakes in continental North America. Organic Geochemistry 66, 38–47.
Marlowe, I.T., Green, J.C., Neal, A.C., Brassell, S.C., Course, P.A., 1984. Long chain (*n*-C_{37}–C_{39}) alkenones in the Prymnesiophyceae. Distribution of alkenones and other lipids and their taxonomic significance. British Phycological Journal 19, 203–216.
M'boule, D., Chivall, D., Sinke-Schoen, D., Sinninghe Damsté, J.S., Schouten, S., van der Meer, M.T., 2014. Salinity dependent hydrogen isotope fractionation in alkenones produced by coastal and open ocean haptophyte algae. Geochimica et Cosmochimica Acta 130, 126–135.
Moros, M., Lemke, W., Kuijpers, A., Endler, R., Jensen, J.B., Bennike, O., Gingele, F., 2002. Regressions and transgressions of the Baltic basin reflected by a new high-resolution deglacial and postglacial lithostratigraphy for Arkona Basin sediments (western Baltic Sea). Boreas 31, 151–162.
Müller, P.J., Kirst, G., Ruhland, G., von Storch, I., Rosell-Melé, A., 1998. Calibration of the alkenone paleotemperature index $U^{K'}_{37}$ based on core-tops from the eastern South Atlantic and the global ocean (60 N–60 S). Geochimica et Cosmochimica Acta 62, 1757–1772.
Ono, M., Sawada, K., Shiraiwa, Y., Kubota, M., 2012. Changes in alkenone and alkenoate distributions during acclimatization to salinity change in *Isochrysis galbana*: implication for alkenone-based paleosalinity and paleothermometry. Geochemical Journal 46, 235–247.
Prahl, F.G., Wakeham, S.G., 1987. Calibration of unsaturation patterns in long-chain ketone compositions for palaeotemperature assessment. Nature 330, 367–369.
Prahl, F.G., Muehlhausen, L.A., Zahnle, D.L., 1988. Further evaluation of long-chain alkenones as indicators of paleoceanographic conditions. Geochimica et Cosmochimica Acta 52, 2303–2310.
Prahl, F.G., Rontani, J.-F., Volkman, J.K., Sparrow, M.A., Royer, I.M., 2006. Unusual C_{35} and C_{36} alkenones in a paleoceanographic benchmark strain of *Emiliania huxleyi*. Geochimica et Cosmochimica Acta 70, 2856–2867.
Punning, J., Martma, T., Kessel, H., Vaikme, R., 1988. The isotopic composition of oxygen and carbon in the subfossil mollusc shells of the Baltic Sea as an indicator of palaeosalinity. Boreas 17, 27–31.
Randlett, M.-E., Coolen, M.J., Stockhecke, M., Pickarski, N., Litt, T., Balkema, C., Kwiecien, O., Tomonaga, Y., Wehrli, B., Schubert, C.J., 2014. Alkenone distribution in Lake Van sediment over the last 270 ka: influence of temperature and haptophyte species composition. Quaternary Science Reviews 104, 53–62.
Rechka, J.A., Maxwell, J.R., 1988. Characterisation of alkenone temperature indicators in sediments and organisms. Organic Geochemistry 13, 727–734.
Rosell-Melé, A., 1998. Interhemispheric appraisal of the value of alkenone indices as temperature and salinity proxies in high-latitude locations. Paleoceanography 13, 694–703.
Ross, D.A., Degens, E.T., MacIlvaine, J., 1970. Black Sea: recent sedimentary history. Science 170, 163–165.
Rößler, D., Moros, M., Lemke, W., 2011. The Littorina transgression in the southwestern Baltic Sea: new insights based on proxy methods and radiocarbon dating of sediment cores. Boreas 40, 231–241.
Ryan, W.B., Pitman, W.C., Major, C.O., Shimkus, K., Moskalenko, V., Jones, G.A., Dimitrov, P., Gorür, N., Sakinç, M., Yüce, H., 1997. An abrupt drowning of the Black Sea shelf. Marine Geology 138, 119–126.
Sachs, J.P., Maloney, A.E., Gregersen, J., Paschall, C., 2016. Effect of salinity on $^2H/^1H$ fractionation in lipids from continuous cultures of the coccolithophorid *Emiliania huxleyi*. Geochimica et Cosmochimica Acta 189, 96–109.
Schouten, S., Ossebaar, J., Schreiber, K., Kienhuis, M.V.M., Langer, G., Bijma, J., 2005. The effect of temperature and salinity on the stable hydrogen isotopic composition of long chain alkenones produced by *Emiliania huxleyi* and *Gephyrocapsa oceanica*. Biogeosciences 2, 1681–1695.
Schulz, H.-M., Schöner, A., Emeis, K.-C., 2000. Long-chain alkenone patterns in the Baltic Sea—an ocean-freshwater transition. Geochimica et Cosmochimica Acta 64, 469–477.
Sikes, E.L., Sicre, M.-A., 2002. Relationship of the tetra-unsaturated C_{37} alkenone to salinity and temperature: implications for paleoproxy applications. Geochemistry, Geophysics, Geosystems 3, 1–11.
Song, M., Zhou, A., He, Y., Zhao, C., Wu, J., Zhao, Y., Liu, W., Liu, Z., 2016. Environmental controls on long-chain alkenone occurrence and compositional patterns in lacustrine sediments, northwestern China. Organic Geochemistry 91, 43–53.
Sun, Q., Chu, G., Liu, G., Li, S., Wang, X., 2007. Calibration of alkenone unsaturation index with growth temperature for a lacustrine species *Chrysotila lamellosa* (Haptophyceae). Organic Geochemistry 38, 1226–1234.
Swart, P.K., 1991. The oxygen and hydrogen isotope composition of the Black Sea. Deep-Sea Research 38, S761–S772.
Thiel, V., Jenisch, A., Landmann, G., Reimer, A., Michaelis, W., 1997. Unusual distributions of long-chain alkenones and tetrahymanol from the highly alkaline Lake Van, Turkey. Geochimica et Cosmochimica Acta 61, 2053–2064.
Tikkanen, M., Oksanen, J., 2002. Late Weichselian and Holocene shore displacement history of the Baltic Sea in Finland. Fennia-International Journal of Geography 180, 9–20.
Theroux, S., D'Andrea, W.J., Toney, J., Amaral-Zettler, L., Huang, Y., 2010. Phylogenetic diversity and evolutionary relatedness of alkenone-producing haptophyte algae in lakes: implications for continental paleotemperature reconstructions. Earth and Planetary Science Letters 300, 311–320.
Theroux, S., Toney, J., Amaral-Zettler, L., Huang, Y., 2013. Production and temperature sensitivity of long chain alkenones in the cultured haptophyte *Pseudoisochrysis paradoxa*. Organic Geochemistry 62, 68–73.
Toney, J.L., Theroux, S., Andersen, R.A., Coleman, A., Amaral-Zettler, L., Huang, Y., 2012. Culturing of the first 37:4 predominant lacustrine haptophyte: geochemical, biochemical, and genetic implications. Geochimica et Cosmochimica Acta 78, 51–64.
van der Meer, M.T., Sangiorgi, F., Baas, M., Brinkhuis, H., Sinninghe Damsté, J.S., Schouten, S., 2008. Molecular isotopic and dinoflagellate evidence for Late Holocene freshening of the Black Sea. Earth and Planetary Science Letters 267, 426–434.
van der Meer, M.T., Benthien, A., Bijma, J., Schouten, S., Sinninghe Damsté, J.S., 2013. Alkenone distribution impacts the hydrogen isotopic composition of the $C_{37:2}$ and $C_{37:3}$ alkan-2-ones in *Emiliania huxleyi*. Geochimica et Cosmochimica Acta 111, 162–166.
van der Meer, M.T., Benthien, A., French, K.L., Epping, E., Zondervan, I., Reichart, G.-J., Bijma, J., Sinninghe Damsté, J.S., Schouten, S., 2015. Large effect of irradiance on hydrogen isotope fractionation of alkenones in *Emiliania huxleyi*. Geochimica et Cosmochimica Acta 160, 16–24.
van Soelen, E.E., Lammers, J.M., Eglinton, T.I., Sinninghe Damsté, J.S., Reichart, G.J., 2014. Unusual C_{35} to C_{38} alkenones in mid-Holocene sediments from a restricted estuary (Charlotte Harbor, Florida). Organic Geochemistry 70, 20–28.
Versteegh, G.J., Riegman, R., de Leeuw, J.W., Jansen, J.F., 2001. $U^{K'}_{37}$ values for *Isochrysis galbana* as a function of culture temperature, light intensity and nutrient concentrations. Organic Geochemistry 32, 785–794.
Volkman, J.K., Eglinton, G., Corner, E.D.S., Forsberg, T.E.V., 1980. Long-chain alkenes and alkenones in the marine coccolithophorid *Emiliania huxleyi*. Phytochemistry 19, 2619–2622.
Volkman, J.K., Burton, H.R., Everitt, D.A., Allen, D.I., 1988. Pigment and lipid compositions of algal and bacterial communities in Ace Lake, Vestfold Hills, Antarctica. Hydrobiologia 165, 41–57.
Volkman, J.K., Barrett, S.M., Blackburn, S.I., Sikes, E.L., 1995. Alkenones in *Gephyrocapsa oceanica*: implications for studies of paleoclimate. Geochimica et Cosmochimica Acta 59, 513–520.
Westman, P., Sohlenius, G., 1999. Diatom stratigraphy in five offshore sediment cores from the northwestern Baltic proper implying large scale circulation changes during the last 8500 years. Journal of Paleolimnology 22, 53–69.
Winterhalter, B., 1992. Late-Quaternary stratigraphy of Baltic Sea basins–a review. Bulletin of the Geological Society Finland 64, 189–194.
Witkowski, A., Broszinski, A., Bennike, O., Janczak-Kostecka, B., Jensen, J.B., Lemke, W., Endler, R., Kuijpers, A., 2005. Darss Sill as a biological border in the fossil record of the Baltic Sea: evidence from diatoms. Quaternary International 130, 97–109.
Wolhowe, M.D., Prahl, F.G., Langer, G., Oviedo, A.M., Ziveri, P., 2015. Alkenone δD as an ecological indicator: a culture and field study of physiologically-controlled chemical and hydrogen-isotopic variation in C_{37} alkenones. Geochimica et Cosmochimica Acta 162, 166–182.
Xu, L., Reddy, C.M., Farrington, J.W., Frysinger, G.S., Gaines, R.B., Johnson, C.G., Nelson, R.K., Eglinton, T.I., 2001. Identification of a novel alkenone in Black Sea sediments. Organic Geochemistry 32, 633–645.
Zheng, Y., Huang, Y., Andersen, R.A., Amaral-Zettler, L.A., 2016. Excluding the di-unsaturated alkenone in the U^{K}_{37} index strengthens temperature correlation for the common lacustrine and brackish-water haptophytes. Geochimica et Cosmochimica Acta 175, 36–46.
Zink, K.-G., Leythaeuser, D., Melkonian, M., Schwark, L., 2001. Temperature dependency of long-chain alkenone distributions in recent to fossil limnic sediments and in lake waters. Geochimica et Cosmochimica Acta 65, 253–265.